Ion Coulomb Crystals

Michael Drewsen

The Ion Trap Group
Department of Physics and Astronomy
Aarhus University

Physics with Trapped Charged Particles
Les Houches, January 16, 2018

Outline:

I. Conditions for Coulomb crystallization

II. Structural properties under various trapping conditions

III. Metastable long-range-ordered Coulomb clusters

IV. Control of crystal structures by light induced forces

I. Conditions for Coulomb crystallization

Conditions for Coulomb crystallization

Condition for the formation of Coulomb crystals

3D, infinite case:

classical

$$\Gamma = E_{Coul}/E_{kin} = Q^2/(4\pi\varepsilon_0 a k_B T) > \sim 170 \quad ,$$

or equivalent

$$a/\Delta r_{kin} > \sim 10$$

with $a=(3/(4\pi n))^{1/3}$ is the Wigner-Seitz radius

J.-P. Hansen, Phys. Rev. A **8**, 3096 (1973)

3D, finite case:

Γ=~200 (~10.000 ions) – 500 (~100 ions)

J. P Schiffer, PRL **88**, 205003(2002)

Historical background

Wigner 1934:

Electrons in metals at low temperatures:

Normally, $\Delta r \sim a$ due to quantum mechanics.

By *lowering* the electron density one would, however, get Coulomb crystals or so-called

Wigner-crystals.

Still not observed in 3D, but….

~1980: 2D Wigner-crystals on the surface of superfluid helium

~1990: 2D Wigner-crystals in GaAs/GaAlAs quantum well stuctures

~2000: Simulations of few electrons in a quantum dot:

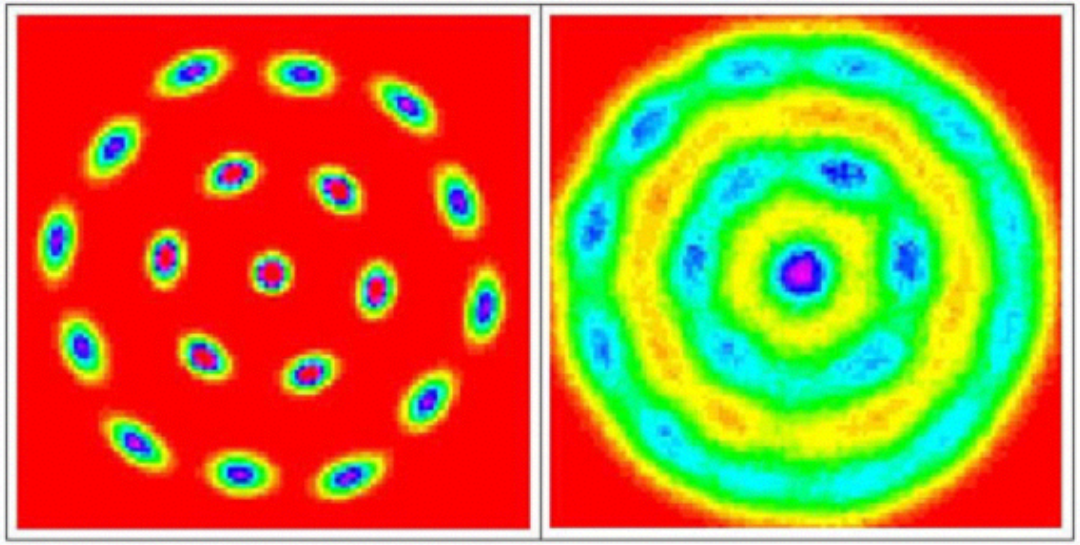

Filinov, Bonitz, Lozovik

What about ions?

~1980:

Dense stellar objects: White Dwarfs and Neutron Stars

Criterion for avoiding "quantum melting":

$$a > 10^4 \times h^2 \varepsilon_0 / (Q^2 m)$$

Interior of WD: C^{6+}, O^{8+} => $a > \sim 10^{-12}$ m
Crust of NS: Fe^{26+} => $a > \sim 10^{-14}$ m

I.e., at sufficient "low" temperatures (~10^6 K) ion Coulomb crystals are expected to be present in these exotic objects !

Trap experiments

<1980:

Trap ion densities of $n \sim 10^8$ cm^{-3} and temperatures of >1 K

=> $\Gamma < 1$

~1980:

First demonstartion of **laser cooling** of ions. (NIST, Hamburg)

=> $\Gamma \sim 1000$

~1980 ->: Non-neutral plasma physics, statistical physics, non-linear dynamics, metrology, quantum optics, cold molecules, nuclear physics, solid state physics...

The linear Paul trap

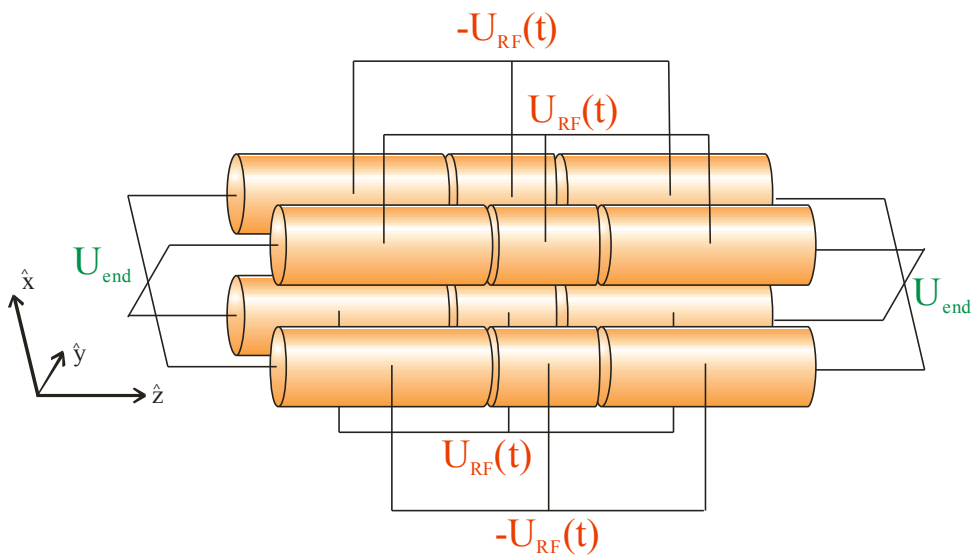

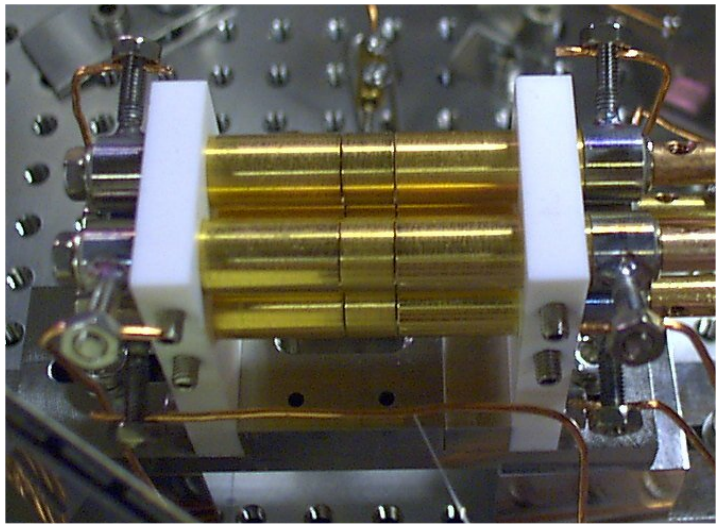

Sinusoidal RF potential: $U_{RF}(t)=U_{RF}\sin(\Omega t)$

Effective oscillation freq.'s:

$\omega_r=1/2\,\beta\,\Omega\,, \quad \beta=(1/2\,q^2+a)^{1/2}$

$\omega_z=(-1/2\,a)^{1/2}\Omega$

$$q=\frac{4QU_{RF}}{m\Omega^2 r_0^2} \qquad a=-\frac{\alpha Q U_{end}}{m\Omega^2 r_0^2}$$

The Aarhus linear Paul trap

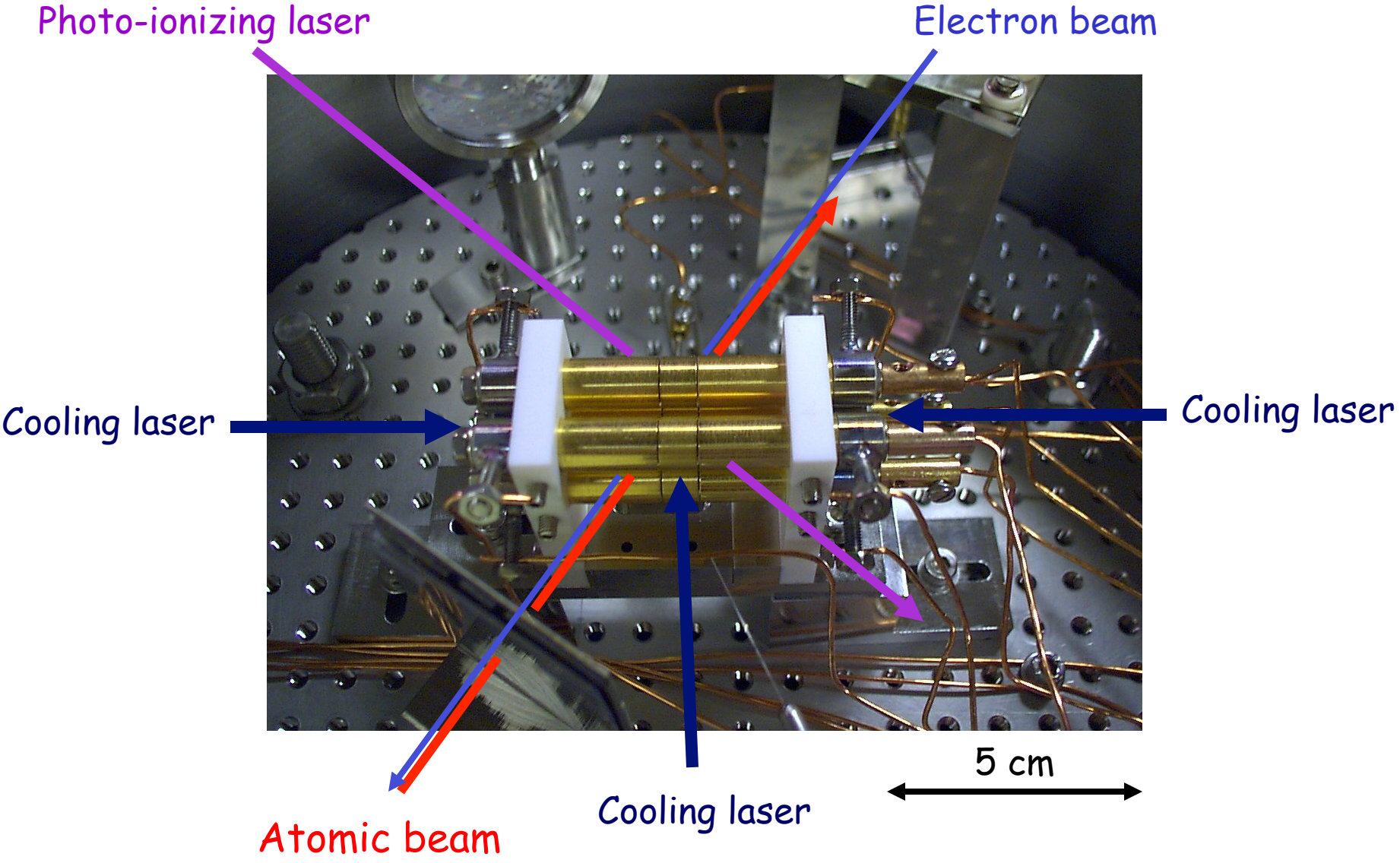

II. Structural properties under various trapping conditions

Single species ion Coulomb crystals

Smaller crystals – strings of ions

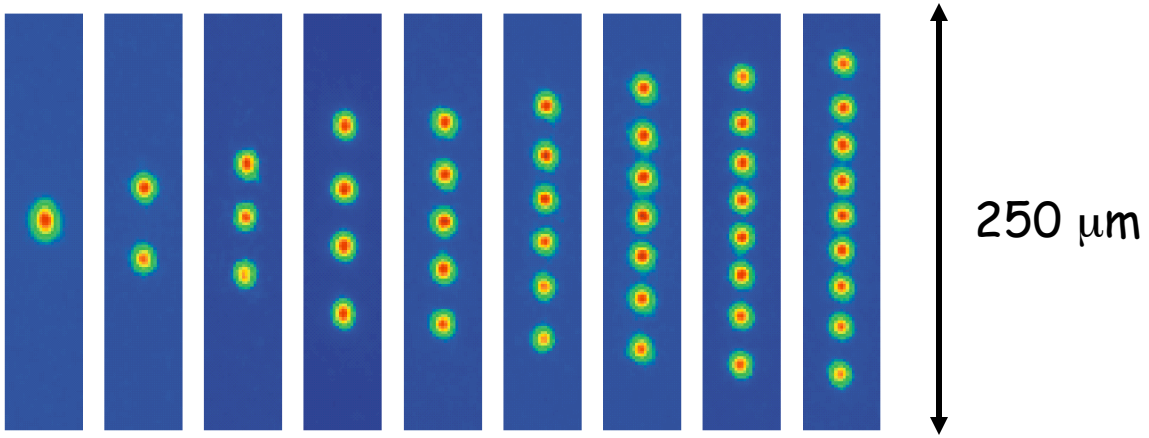

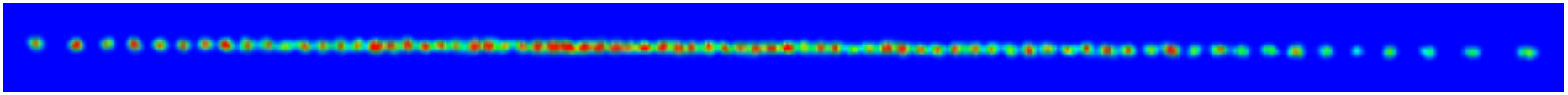

1 mm

Ion spacing: ~ 10 μm

How to determine the 1D linear ion structure?

Potential energy:

$$V = \sum_{m=1}^{N} \frac{1}{2} M v^2 x_m(t)^2 + \sum_{\substack{n,m=1 \\ m \neq n}}^{N} \frac{Z^2 e^2}{8\pi\epsilon_0} \frac{1}{|x_n(t) - x_m(t)|}$$

Equilibrium positions:

$$\left[\frac{\partial V}{\partial x_m} \right]_{x_m = x_m^{(0)}} = 0$$

James, Appl. Phys. B **66**, 181 (1998)

Scaled equilibrium positions

N										
2					−0.62996		0.62996			
3				−1.0772		0		1.0772		
4			−1.4368		−0.45438		0.45438		1.4368	
5		−1.7429		−0.8221		0		0.8221		1.7429
6	−2.0123		−1.1361		−0.36992		0.36992		1.1361		2.0123
7		−2.2545		−1.4129		−0.68694	0	0.68694		1.4129		2.2545
8	−2.4758		−1.6621		−0.96701		−0.31802		0.31802		0.96701		1.6621		2.4758
9		−2.6803		−1.8897		−1.2195		−0.59958	0	0.59958		1.2195		1.8897		2.6803
10	−2.8708		−2.10003		−1.4504		−0.85378		−0.2821		0.2821		0.85378		1.4504		2.10003		2.8708

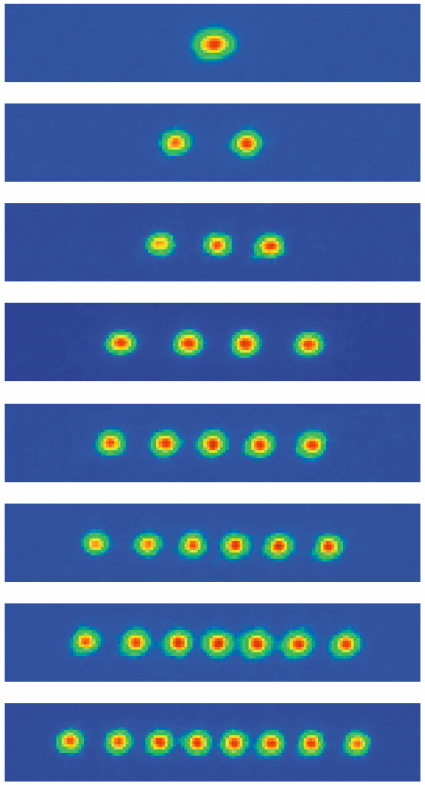

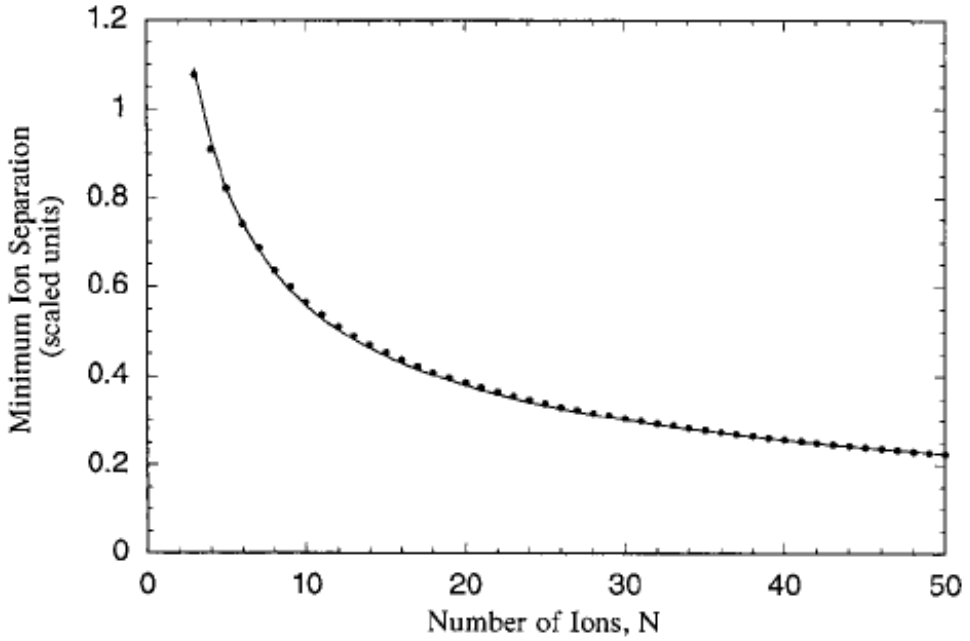

James, Appl. Phys. B **66**, 181 (1998)

Normal mode frequencies and eigenvectors

#ions $\omega_{N,i}^2$:

N=2	1	(0.7071,	0.7071)				
	3	(−0.7071,	0.7071)				
N=3	1	(0.5774,	0.5774,	0.5774)			
	3	(−0.7071,	0,	0.7071)			
	5.8	(0.4082,	−0.8165,	0.4082)			
N=4	1	(0.5,	0.5,	0.5,	0.5)		
	3	(−0.6742,	−0.2132,	0.2132,	0.6742)		
	5.81	(0.5,	−0.5,	−0.5,	0.5)		
	9.308	(−0.2132,	0.6742,	−0.6742,	0.2132)		
N=5	1	(0.4472,	0.4472,	0.4472,	0.4472,	0.4472)	
	3	(−0.6395,	−0.3017,	0,	0.3017,	0.6395)	
	5.818	(0.5377,	−0.2805,	−0.5143,	−0.2805,	0.5377)	
	9.332	(−0.3017,	0.6395,	0,	−0.6395,	0.3017)	
	13.47	(0.1045,	−0.4704,	0.7318,	−0.4704,	0.1045)	
N=6	1	(0.4082,	0.4082,	0.4082,	0.4082,	0.4082,	0.4082)
	3	(−0.608,	−0.3433,	−0.1118,	0.1118,	0.3433,	0.608)
	5.824	(−0.5531,	0.1332,	0.4199,	0.4199,	0.1332,	−0.5531)
	9.352	(0.3577,	−0.5431,	−0.2778,	0.2778,	0.5431,	−0.3577)
	13.51	(0.1655,	−0.5618,	0.3963,	0.3963,	−0.5618,	0.1655)
	18.27	(−0.04902,	0.2954,	−0.6406,	0.6406,	−0.2954,	0.04902)
N=7	1	(0.378,	0.378,	0.378,	0.378,	0.378,	0.378,	0.378)
	3	(−0.5801,	−0.3636,	−0.1768,	0,	0.1768,	0.3636,	0.5801)
	5.829	(−0.5579,	0.031,	0.3213,	0.4111,	0.3213,	0.031,	−0.5579)
	9.369	(−0.3952,	0.445,	0.3818,	0,	−0.3818,	−0.445,	0.3952)
	13.55	(−0.213,	0.5714,	−0.1199,	−0.4769,	−0.1199,	0.5714,	−0.213)
	18.32	(0.08508,	−0.4121,	0.5683,	0,	−0.5683,	0.4121,	−0.08508)
	23.66	(0.02222,	−0.1723,	0.4894,	−0.6787,	0.4894,	−0.1723,	0.02222)

James, Appl. Phys. B **66**, 181 (1998)

Medium size crystals (~100 - ~1000 ions)

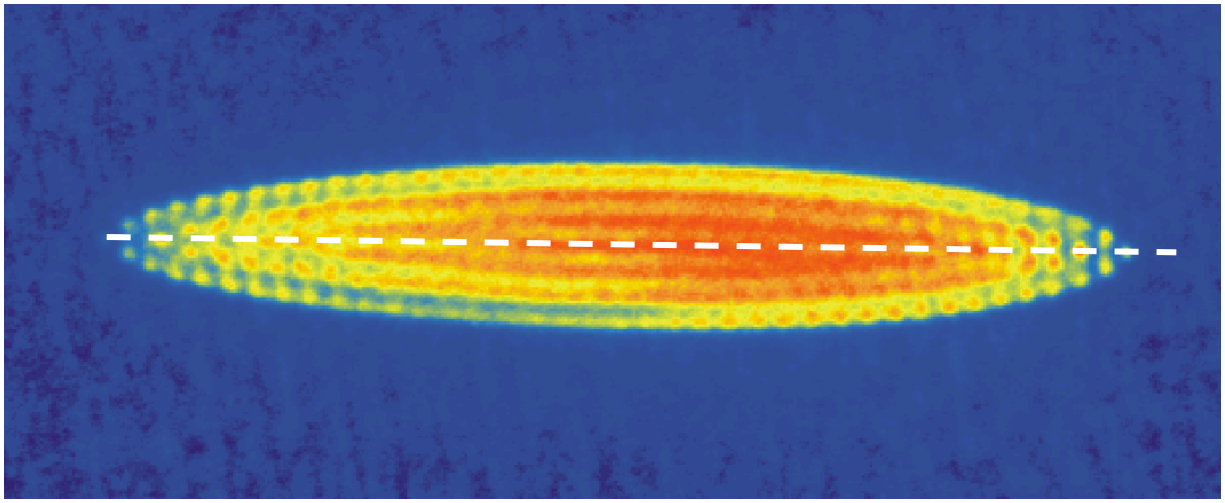

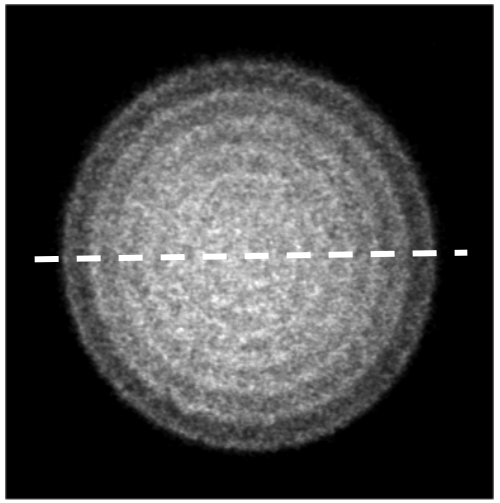

Properties:

Shells with near-hexagonal structures

Uniform density of ~10^8 cm^{-3}

Temperature of ~10 mK

Trap life times of hours @ P~10^{-10} mBar

Outer contours of crystals

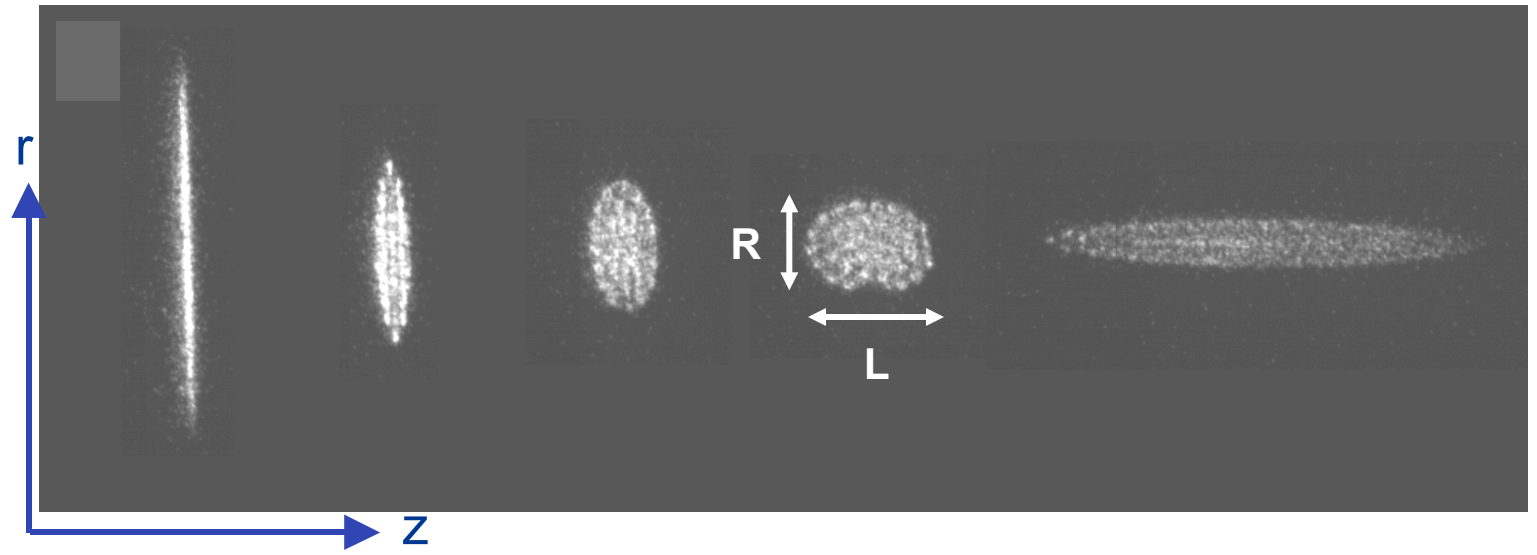

Cold uniformly charged liquid model

In the oblate case, $\alpha = R/L > 1$,

$$\frac{\omega_z^2}{\omega_r^2} = -2\frac{\sin^{-1}(1-\alpha^{-2})^{1/2} - \alpha(1-\alpha^{-2})^{1/2}}{\sin^{-1}(1-\alpha^{-2})^{1/2} - \alpha^{-1}(1-\alpha^{-2})^{1/2}},$$

and in the prolate case, $\alpha = R/L < 1$,

$$\frac{\omega_z^2}{\omega_r^2} = -2\frac{\sinh^{-1}(\alpha^{-2}-1)^{1/2} - \alpha(\alpha^{-2}-1)^{1/2}}{\sinh^{-1}(\alpha^{-2}-1)^{1/2} - \alpha^{-1}(\alpha^{-2}-1)^{1/2}}.$$

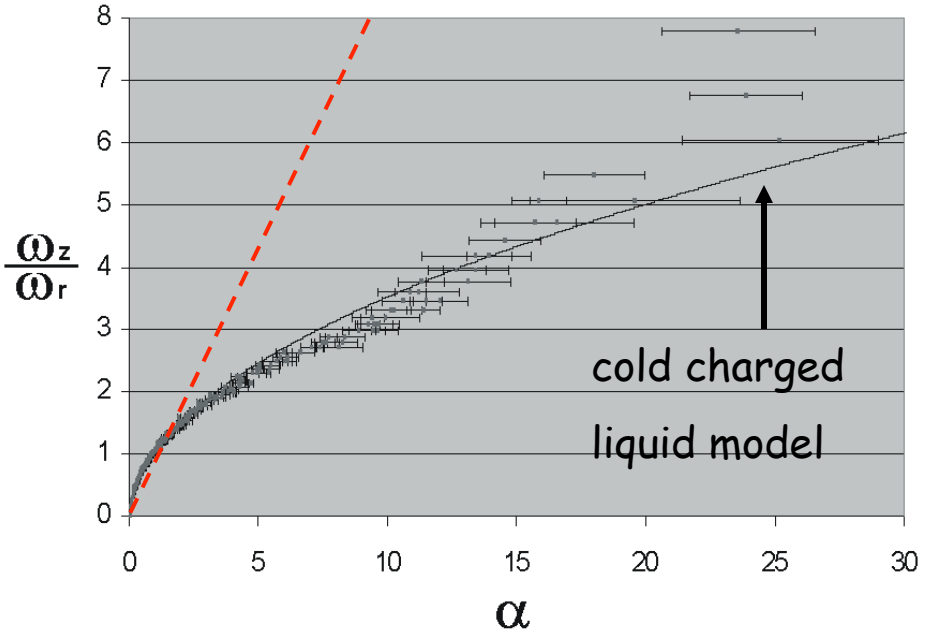

L. Turner, Phys. Fluids **30**, 3196 (1987)

Control of the conformations of ion Coulomb crystals in a Penning trap

Sandeep Mavadia[1], Joseph F. Goodwin[1], Graham Stutter[1], Shailen Bharadia[1], Daniel R. Crick[1], Daniel M. Segal[1] & Richard C. Thompson[1]

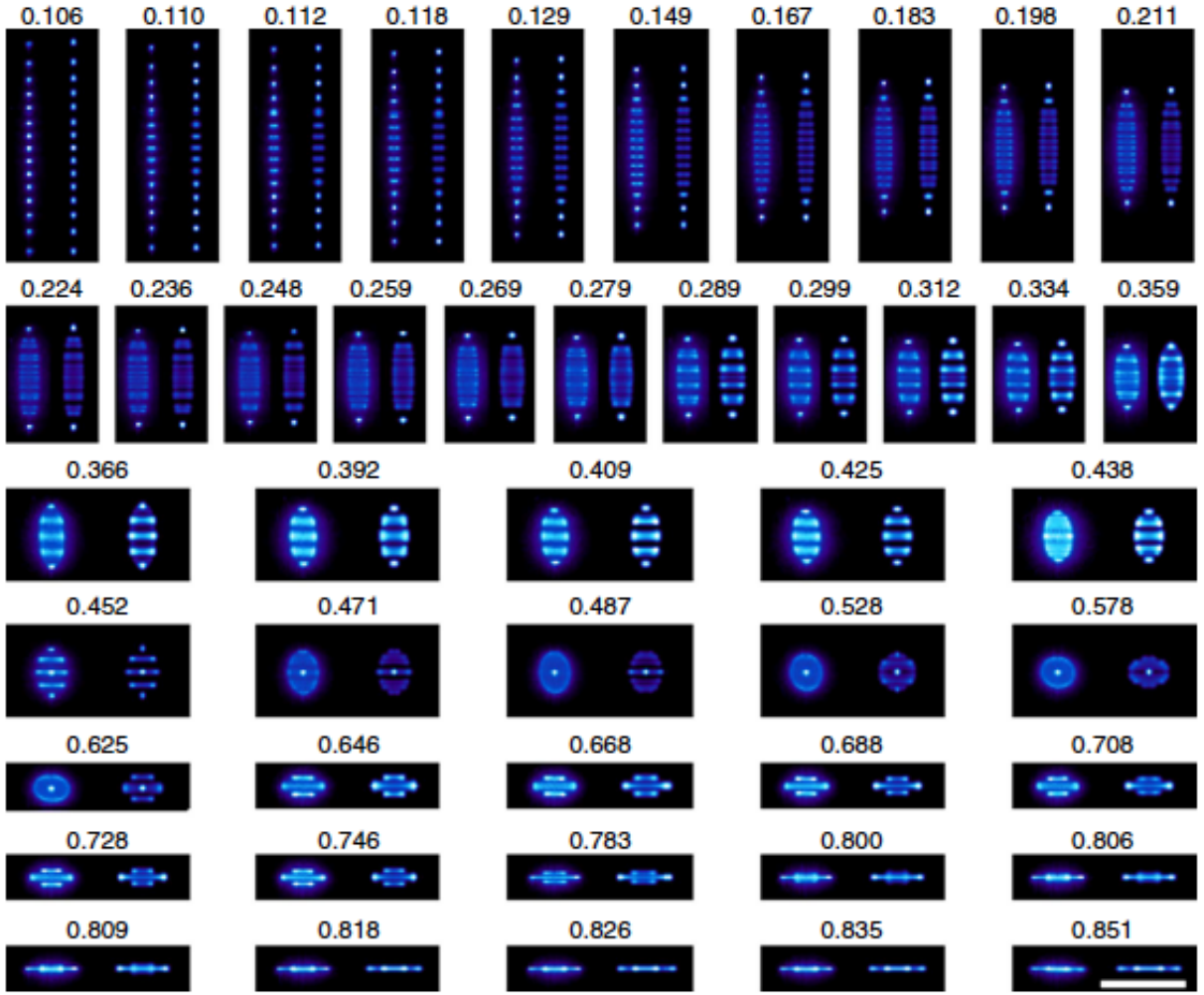

Received 31 May 2013 | Accepted 6 Sep 2013 | Published 7 Oct 2013

DOI: 10.1038/ncomms3571

OPEN

PHYSICAL REVIEW A VOLUME 44, NUMBER 7 1 OCTOBER 1991

Structure and Madelung energy of spherical Coulomb crystals

R. W. Hasse
ESR Division, Gesellschaft für Schwerionenforschung GSI, D-6100 Darmstadt, Germany

V. V. Avilov
ESR Division, Gesellschaft für Schwerionenforschung GSI, D-6100 Darmstadt, Germany
and L.D. Landau Institute for Theoretical Physics, SU-117334 Moscow, U.S.S.R.
(Received 26 March 1991)

$$\mathbf{F}^i_{\text{conf}} = -K\mathbf{r}_i \ ,$$

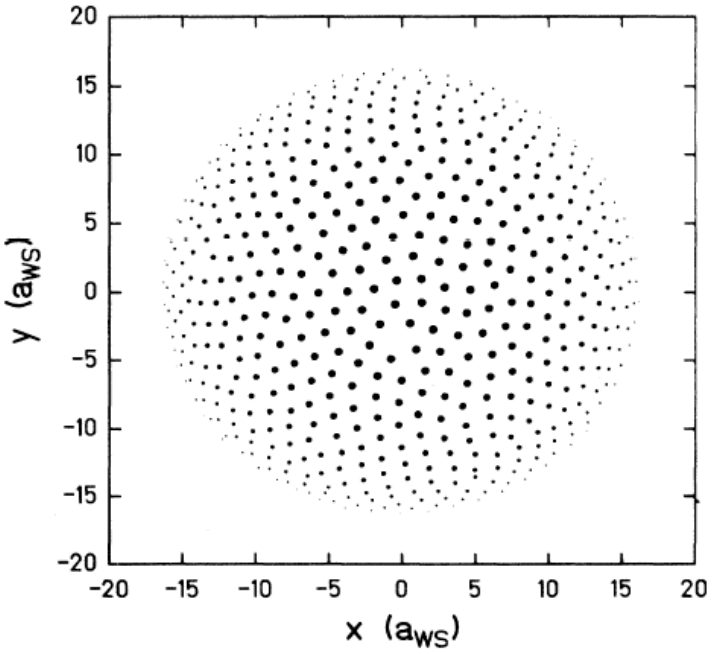

FIG. 1. The front hemisphere of the outer shell of the 5000-ion system. Note the haxagonal structure with approximately equilateral triangles and the point defect below the center.

Ref: PRA **44** 4506 (1991)

TABLE I. Structures ($N_M + N_{M-1} + \cdots + N_1$ particles in subshells), rms radii, and energies of N-particle systems.

N	Structure	$R_{\rm rms}$	ε	Γ
2	2	0.6300	0.5953	∞[a]
3	3	0.8327	1.0400	∞[a]
4	4	0.9721	1.4174	∞[a]
5	5	1.0901	1.7820	10^5
6	6	1.1850	2.1065	10^5
7	7	1.2736	2.4321	10^5
8	8	1.3500	2.7331	10^5
9	9	1.4198	3.0238	10^5
10	10	1.4846	3.3058	10^5
11	11	1.5453	3.5822	10^5
12	12	1.6002	3.8407	10^5
13	12+1	1.6535	4.1009	10^5
26	24+2	2.1633	7.0197	10^5
27	24+3	2.1941	7.2206	10^5
28	24+4	2.2241	7.4200	10^5
29	26+3	2.2532	7.6162	10^5
60	48+12	2.9335	12.9085	10^5
61	48+12+1	2.9511	13.0611	10^5
900	356+247+154+92+38+12+1	7.4389	83.0047	10^6
923	361+253+160+93+43+12+1	7.5023	84.4277	10^7
1024	390+275+108+111+53+16+1	7.7696	90.5438	10^6
1200	448+309+212+132+70+25+4	8.1952	100.7410	10^6
1370	482+354+245+155+91+35+8	8.5683	110.1259	10^6
1415	491+365+244+163+94+44+13+1	8.6619	112.5436	10^7
1600	538+398+285+185+115+58+19+2	9.0270	122.2270	10^6
2000	633+470+357+246+163+85+40+6	9.7287	141.1975	10^6
2057	641+491+363+257+158+93+44+10	9.8209	144.6764	10^8
2837	805+634+480+356+246+173+*143*[b]	10.9384	179.4717	10^7
2869	808+644+482+361+249+165+*160*[b]	10.9796	180.8258	10^8
3816	986+793+618+481+*938*[b]	12.0798	218.8847	10^7
3871	992+801+639+*1439*[b]	12.1379	220.9917	10^8
5000	1183+980+802+*2035*[b]	13.2229	262.2696	10^9

"Magic numbers"

Ref: PRA **44** 4506 (1991)

3D Long-range-order in Coulomb crystals

Theory: Wigner, Hansen, Pollock, Dubin, Hasse, Totsuji ..

Recent MD simulations:

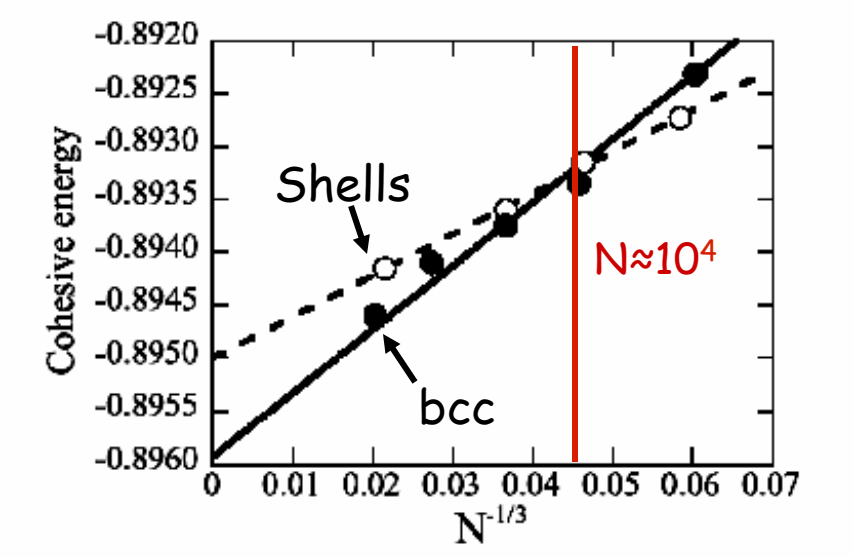

$U_{coh}=\Delta U_{sys}/(Nq^2/a)$

Ref: PRL **88** 125002 (2002)

Bragg Diffraction from Crystallized Ion Plasmas

W. M. Itano,* J. J. Bollinger, J. N. Tan,† B. Jelenković,‡
X.-P. Huang, D. J. Wineland

Penning trap experiments with ~10^5 $^9Be^+$ ions

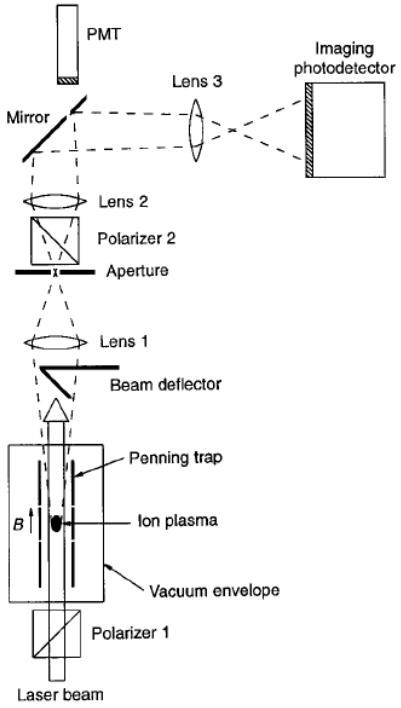

Fig. 1. Experimental setup. Laser light is directed through the ion plasma in the Penning trap. A diffraction pattern is created at a plane beyond lens 2, where rays that are parallel leaving the plasma are focused to a point. A mirror, placed near that plane, deflects the light to an imaging photodetector. An aperture placed inside a hole in the mirror allows diffracted light to be detected by a photomultiplier tube (PMT). The aperture is placed off the axis of the optical system, so the PMT generates a timing signal as the diffraction pattern rotates.

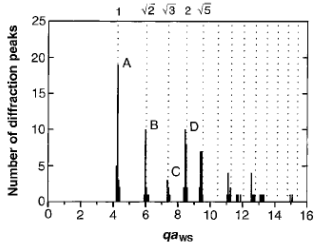

Fig. 3. Histogram representing the numbers of peaks (not intensities) observed as a function of qa_{WS}, where $\mathbf{q} = \mathbf{k}_s - \mathbf{k}_i$ is the difference between the incident ($\mathbf{k}_i$) and scattered ($\mathbf{k}_s$) photon wave vectors. We analyzed 30 Bragg diffraction patterns from two approximately spherical plasmas having 270,000 and 470,000 ions. The dotted lines show the expected peak positions, normalized to the center of gravity of the peak at A ({110} Bragg reflections).

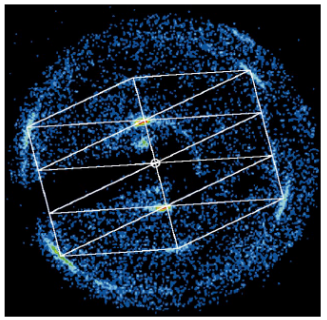

Fig. 5. A Bragg diffraction pattern with twofold symmetry. It matches the pattern expected for a bcc lattice oriented along a ⟨115⟩ direction. A diffraction spot is predicted at each intersection of the grid lines. The passive timing method and the MCP-RA detector were used. Here, $\omega_r = 2\pi \times 149$ kHz, $n_0 = 4.53 \times 10^8$ cm^{-3}, $N = 4 \times 10^5$, $\alpha = 1.20$, and $2r_0 = 1.12$ mm.

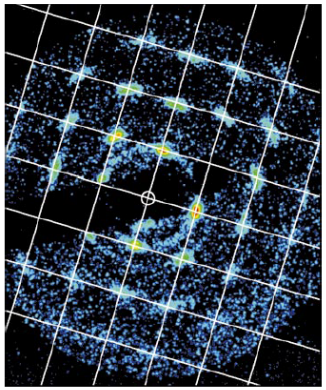

Fig. 4. Time-resolved Bragg diffraction pattern of the same plasma as in Fig. 2. Here and in Figs. 5 and 6 the small open circle marks the position of the undeflected laser beam. A bcc lattice, aligned along a ⟨100⟩ axis, would generate a spot at each intersection of the grid lines overlaid on the image. The grid spacing corresponds to an angular deviation of 2.54×10^{-2} rad. Here, $\omega_r = 2\pi \times 125.6$ kHz, $n_0 = 3.83 \times 10^8$ cm^{-3}, $N = 5 \times 10^5$, $\alpha = 0.98$, and $2r_0 = 1.36$ mm.

W. M. Itano *et al.*, Science **279**, 686 (1998)

Direct Observations of Structural Phase Transitions in Planar Crystallized Ion Plasmas

T. B. Mitchell,* J. J. Bollinger, D. H. E. Dubin, X.-P. Huang,
W. M. Itano, R. H. Baughman

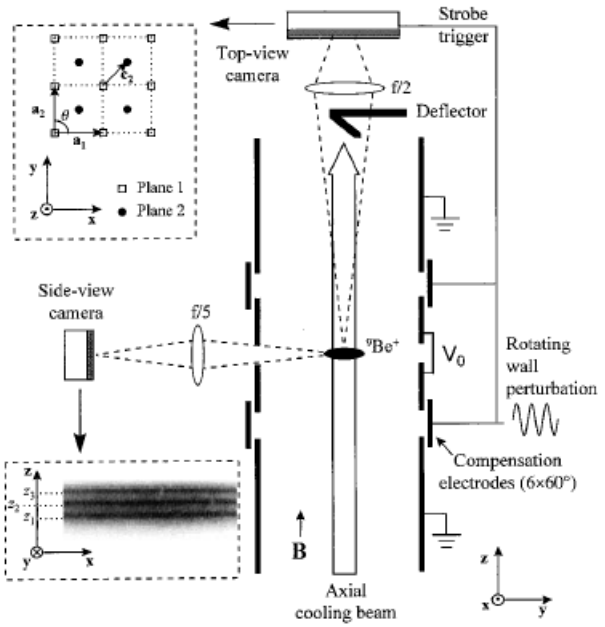

Fig. 1. Schematic side view of the cylindrical Penning trap with its side- and top-view imaging optics. The insets show the variables used to characterize the intra- and interlayer structure. The side-view inset also shows the central region of a lenticular ion plasma with three axial lattice planes. The rotation frequency of the ion plasma was controlled by applying properly phased sinusoidally time-varying electric potentials to the sixfold azimuthally segmented compensation electrodes.

Table 1. Primitive and interlayer displacement vectors in the (x, y) plane for the observed phases. The primitive vector $\mathbf{a}_1$ defines the $\hat{\mathbf{x}}$ direction, and $|\mathbf{a}_1| = |\mathbf{a}_2| = a$. Dashes, not applicable.

Phase	Symmetry	Stacking	Vectors			
			$\mathbf{a}_1$	$\mathbf{a}_2$	$\mathbf{c}_2$	$\mathbf{c}_3$
I	Hexagonal	Single plane	$(a, 0)$	$(a \cos 60°, a \sin 60°)$	—	—
III	Square	Staggered	$(a, 0)$	$(0, a)$	$(\mathbf{a}_1 + \mathbf{a}_2)/2$	$(0, 0)$
IV	Rhombic	Staggered	$(a, 0)$	$(a \cos\theta, a \sin\theta)$	$(\mathbf{a}_1 + \mathbf{a}_2)/2$	$(0, 0)$
V	Hexagonal	hcp-like	$(a, 0)$	$(a \cos 60°, a \sin 60°)$	$(\mathbf{a}_1 + \mathbf{a}_2)/3$	$(0, 0)$
V_{fcc}	Hexagonal	fcc-like	$(a, 0)$	$(a \cos 60°, a \sin 60°)$	$(\mathbf{a}_1 + \mathbf{a}_2)/3$	$2(\mathbf{a}_1 + \mathbf{a}_2)/3$

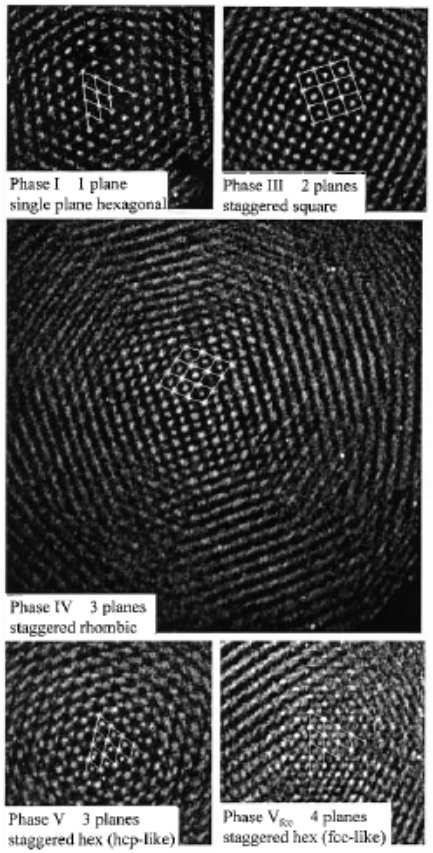

Fig. 2. Top-view (x, y) images of the five structural phases observed in the experiment, with lines showing a fit of the central ions to the indicated structure.

ANNALS OF PHYSICS 203, 419–448 (1990)

The Structure of the Cylindrically Confined Coulomb Lattice

R. W. HASSE

Gesellschaft für Schwerionenforschung GSI, D-6100 Darmstadt, Germany

AND

J. P. SCHIFFER

Argonne National Laboratory, Argonne, Illinois 60439-4843, and
University of Chicago, Chicago, Illinois 60637

Received February 27, 1990

For an infinitely long cylinder of radius R_0 with a charge density σ per unit length the repulsive Coulomb force for particles with charge q is

$$F_{\text{int}} = 2q\sigma \begin{cases} r/R_0^2, & r < R_0 \\ 1/r, & r > R_0 \end{cases} \tag{1.1}$$

and with the external confining (focusing) force

$$\mathbf{F}_{\text{conf}} = -qK\mathbf{r} \tag{1.2}$$

the equilibrium condition is that

$$F_{\text{conf}} + F_{\text{int}} = 2\sigma q/R_0^2 - qK \equiv 0 \tag{1.3}$$

yielding

$$R_0 = \sqrt{2\sigma/K}. \tag{1.4}$$

tions of infinite one-component plasmas [7, 8]. Outside the cylinder, for $r > R_0$ there is, of course, an increasing radial restoring force

$$F_{\text{tot}} = -qK(r - R_0^2/r). \tag{1.5}$$

The average density on the inside of the cylinder being uniform, the average volume per particle is $\pi R_0^2 q/\sigma = 2\pi q/K$, and setting this equal to a volume of $4\pi a^3/3$ yields a Wigner–Seitz radius,

$$a = \left(\frac{3q}{2K}\right)^{1/3}. \tag{1.6}$$

Note that the average distance between neighbouring ions in large systems is almost twice this value. In units of a we define the dimensionless linear particle density

$$\lambda \equiv \sigma a/q \tag{1.7}$$

Ann. Phys. 203, 419 (1990)

The structure of cylindrically confined infinite crystals

Projections to the radial plane

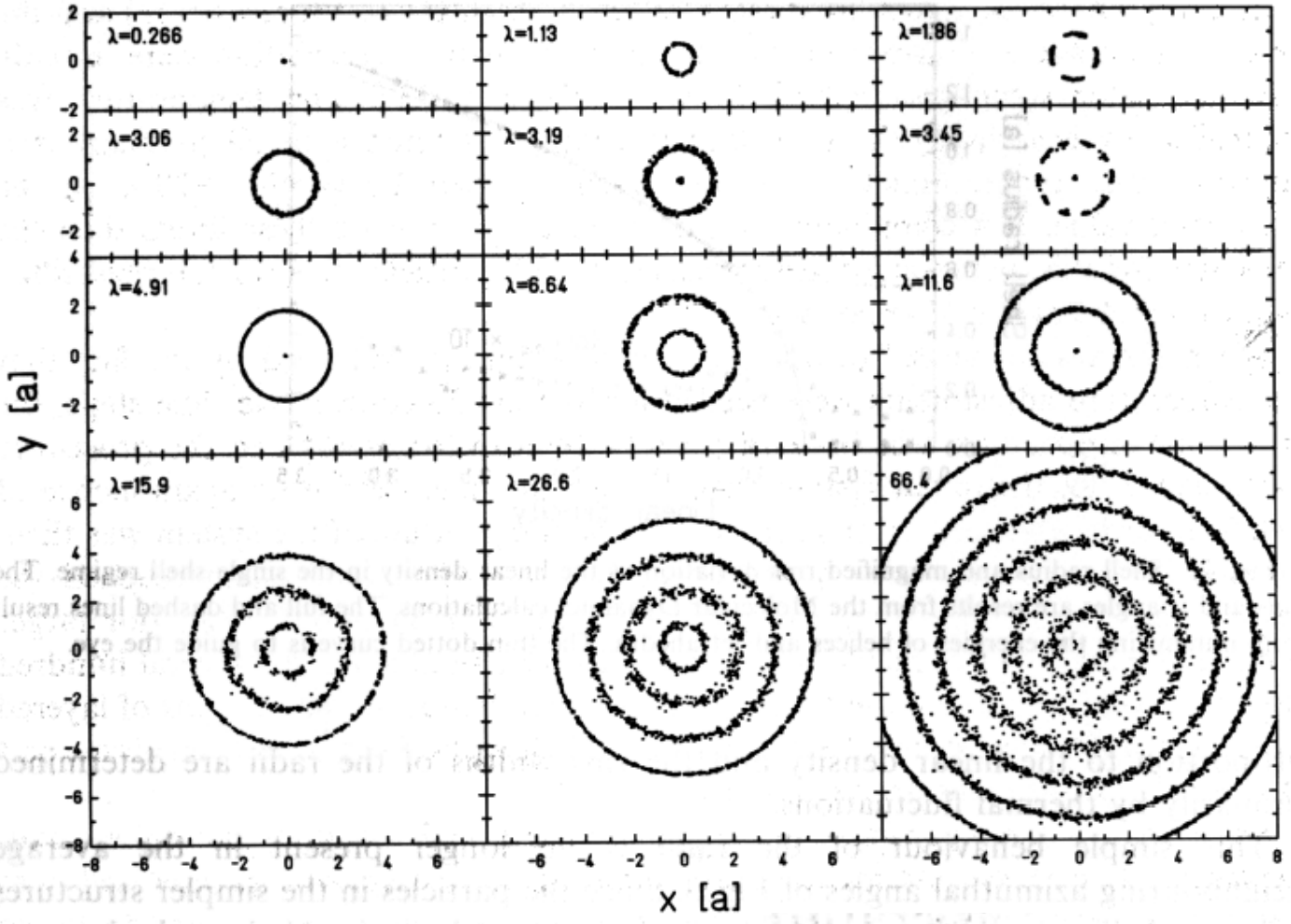

Dimensionless linear charge density: $\lambda \equiv \sigma a/q$

Hasse and Schiffer, Ann. Phys. **203**, 419 (1990)

The structure of cylindrically confined infinite crystals

Structures for increasing linear densities

Total linear density	Structure
$0 < \lambda < 0.709$	String
$0.709 < \lambda < 0.964$	Zigzag
$0.964 < \lambda < 1.25$	1st Helix solution
$1.25 < \lambda < 1.39$	Tetrahedron
$1.39 < \lambda < 1.70$	1st Helix solution
$1.70 < \lambda < 2.19$	Tetrahedron
$2.19 < \lambda < 2.52$	2nd Helix solution
$2.52 < \lambda < 2.96$	Helix
$2.96 < \lambda < 3.10$	3rd Helix solution
$3.10 < \lambda < 5.7$	Shell + string
$5.7 < \lambda < 9.5$	2 Shells
$9.5 < \lambda < 13$	2 Shells + string
$\lambda = 19.9$	3 Shells + string
$\lambda = 26.6$	4 Shells
$\lambda = 66.4$	6 Shells

Hasse and Schiffer, Ann. Phys. **203**, 419 (1990)

Observation of multi-shell structures in a quadrupole storage ring

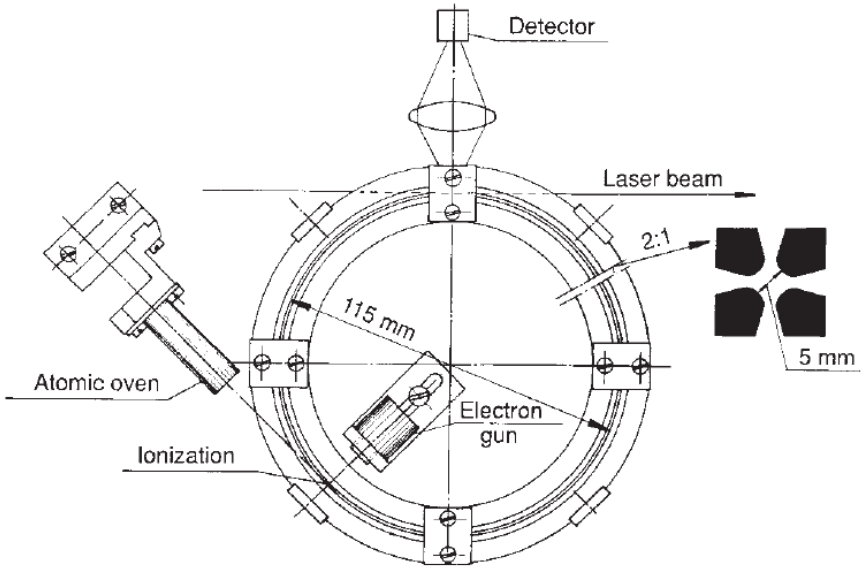

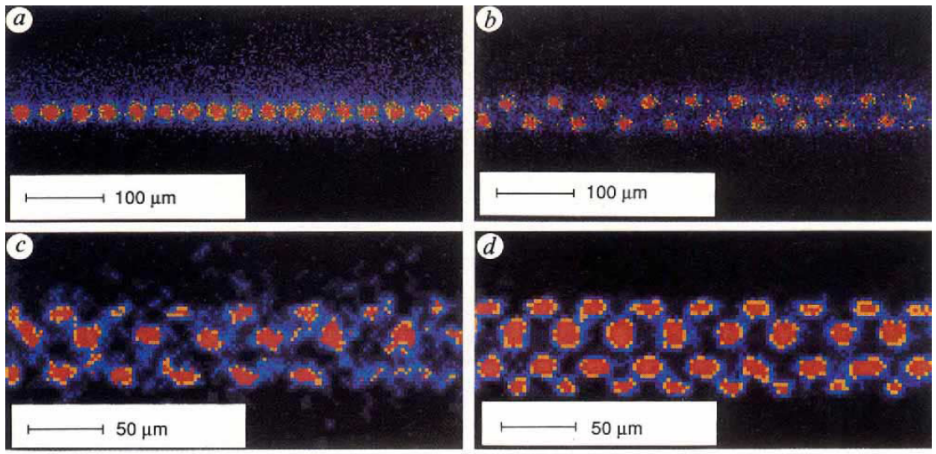

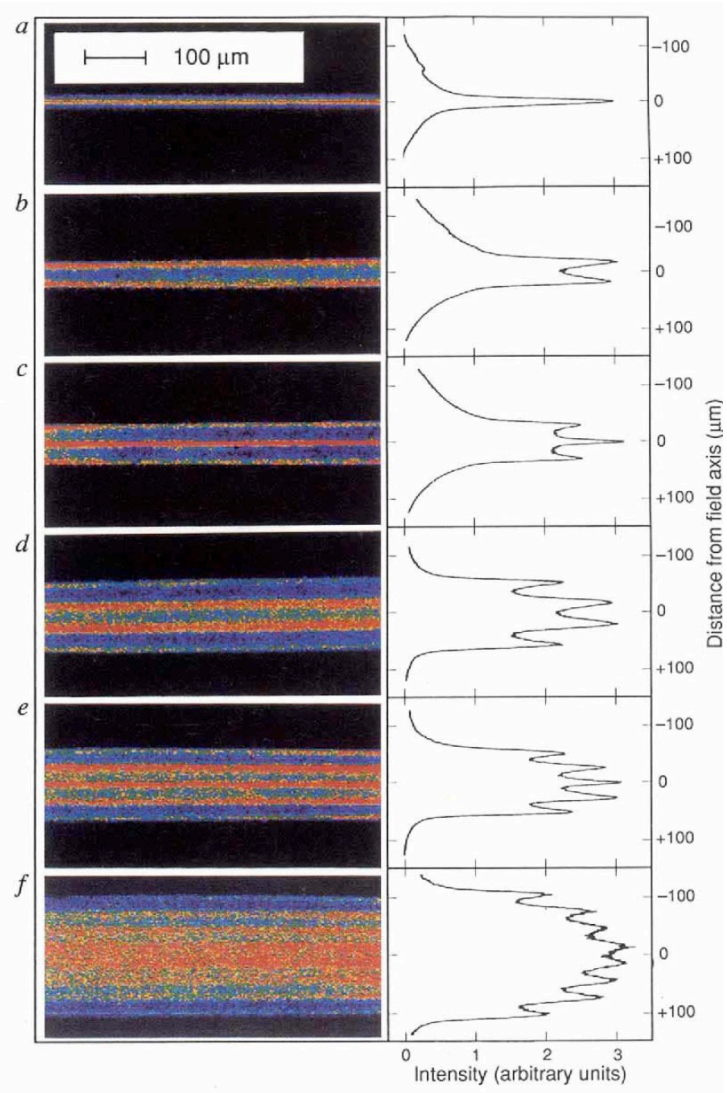

G. Birkl, S. Kassner & H. Walther

NATURE · VOL 357 · 28 MAY 1992

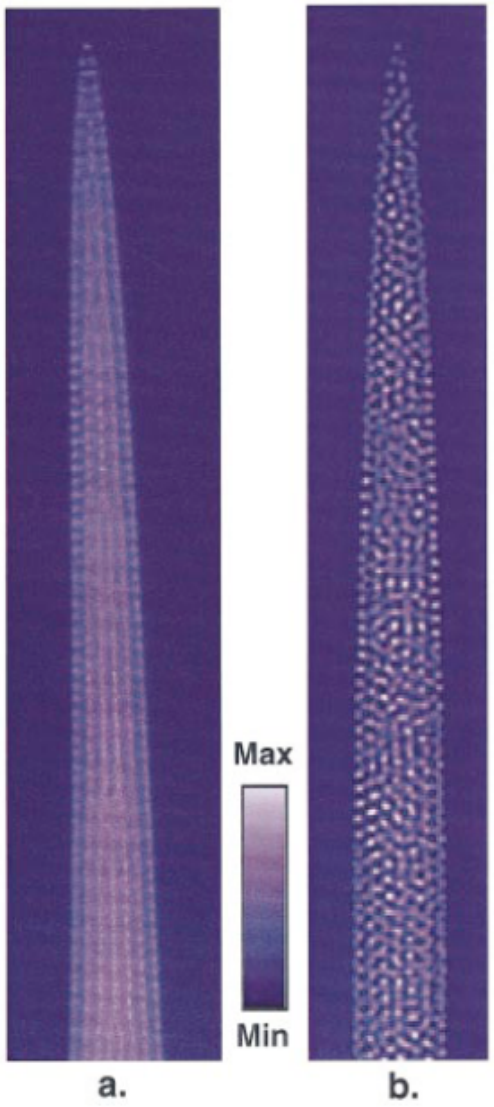

FIG. 1(color). (a) CCD picture integrated over 2 sec of a very prolate crystal of about 3500 ions. (b) Molecular dynamic simulation with 3500 ions in a crystal with roughly the same aspect ratio as the one in (a).

Large Ion Crystals in a Linear Paul Trap

M. Drewsen, C. Brodersen, L. Hornekær, and J. S. Hangst
Institute of Physics and Astronomy, University of Aarhus, DK-8000 Aarhus, Denmark

J. P. Schifffer
Argonne National Laboratory, Argonne, Illinois 60439
and University of Chicago, Chicago, Illinois 60637
(Received 5 December 1997)

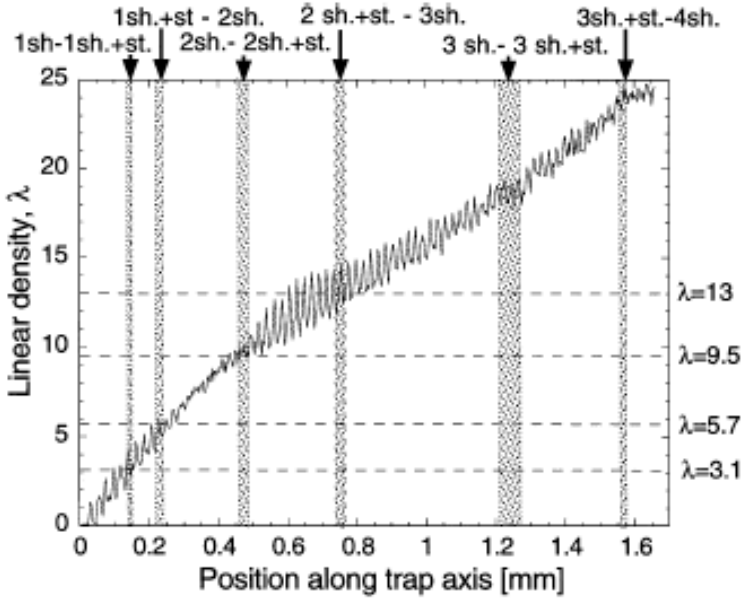

FIG. 2. The dimensionless linear density λ as a function of position along the crystal is shown in Fig. 1a (solid line). The shaded vertical areas indicate the uncertainties in the measured position of structural transitions, while the dashed horizontal lines correspond to linear densities where these transitions should happen according to MD simulation for infinite long crystals.

Ref: PRL **81** 2878 (1998)

Two-species ion Coulomb crystals

Effective oscillation freq.'s:

$\omega_r = 1/2\,\beta\,\Omega\,, \quad \beta = (1/2\,q^2 + a)^{1/2}$

$\omega_z = (-1/2\,a)^{1/2}\,\Omega$

$$q = \frac{4Q\,U_{RF}}{m\Omega^2 r_0^{\,2}} \qquad a = -\frac{\alpha Q\,U_{end}}{m\Omega^2 r_0^{\,2}}$$

Atomic density:

$$n_i = (\epsilon_0 U_{\mathrm{rf}}^2)/(M_i r_0^4 \Omega^2)$$

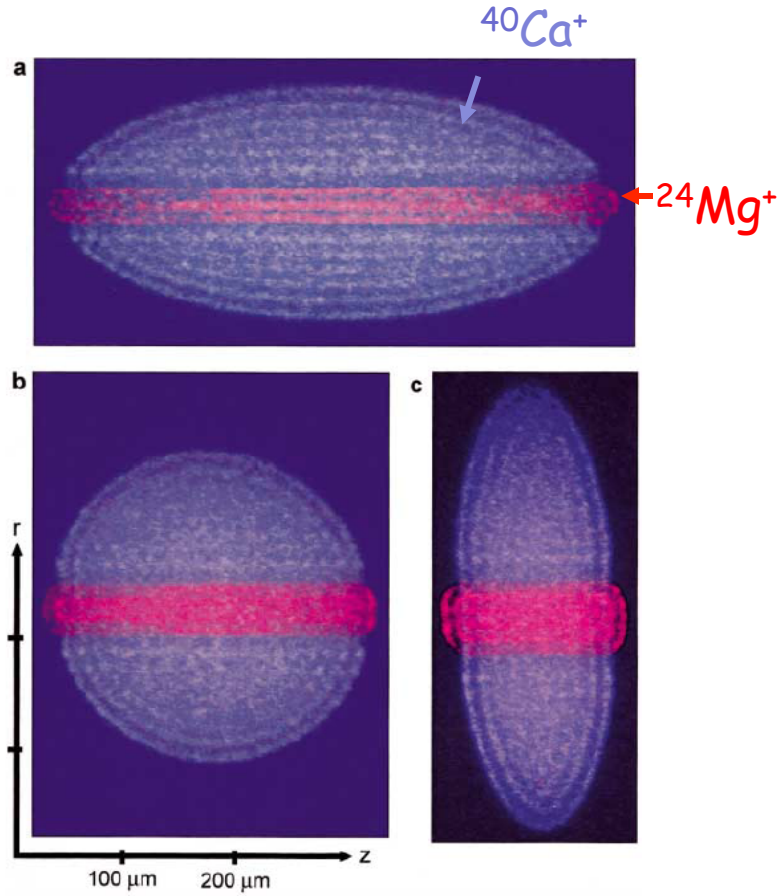

FIG. 2 (color). A $^{40}Ca^+/^{24}Mg^+$ bicrystal at three different end cap voltages. The crystal is symmetric under rotations around the trap axis, z, and contains approximately 300 $^{24}Mg^+$ ions (red) and 3000 $^{40}Ca^+$ ions (blue). The ratios of the axial and effective radial trapping frequencies for $^{40}Ca^+$ and $^{24}Mg^+$ ions in the three cases shown are (a) $\omega_{z,Mg^+}/\omega_{r,Mg^+} = 0.4$ and $\omega_{z,Ca^+}/\omega_{r,Ca^+} = 0.6$; (b) $\omega_{z,Mg^+}/\omega_{r,Mg^+} = 0.7$ and $\omega_{z,Ca^+}/\omega_{r,Ca^+} = 1.0$; (c) $\omega_{z,Mg^+}/\omega_{r,Mg^+} = 1.1$ and $\omega_{z,Ca^+}/\omega_{r,Ca^+} = 1.8$.

Ref: PRL **86** 1994 (2001)

~3000 $^{40}Ca^{+}$ + 47 $^{24}Mg^{+}$

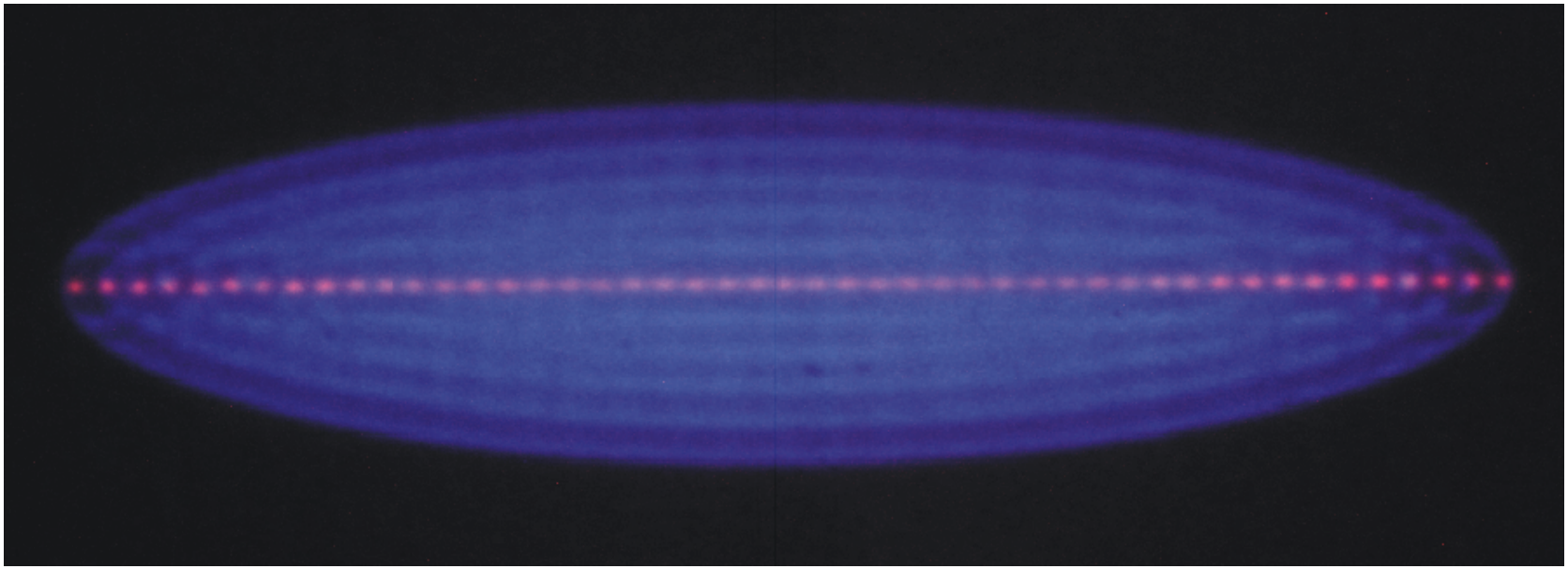

Equidistantly spaced ions in the string!

Similar to an infinite long single component crystal!

Ref: PRL **86** 1994 (2001)

Coulomb crystals of two species with the same charge-to mass ratio

Simulations: 50:50 systems with $q_2=2q_1$, $m_2=2m_1$

Full mixing and double shells

Radial density distributions

20,288 ions

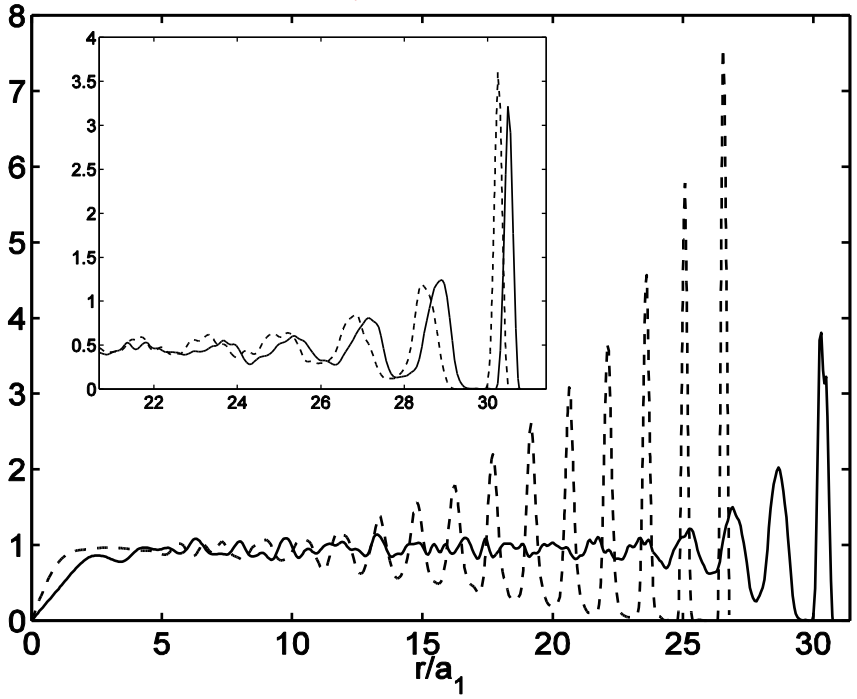

$$n_i = (\epsilon_0 U_{\rm rf}^2)/(M_i r_0^4 \Omega^2)$$

Ground state vs. $N^{-1/3}$

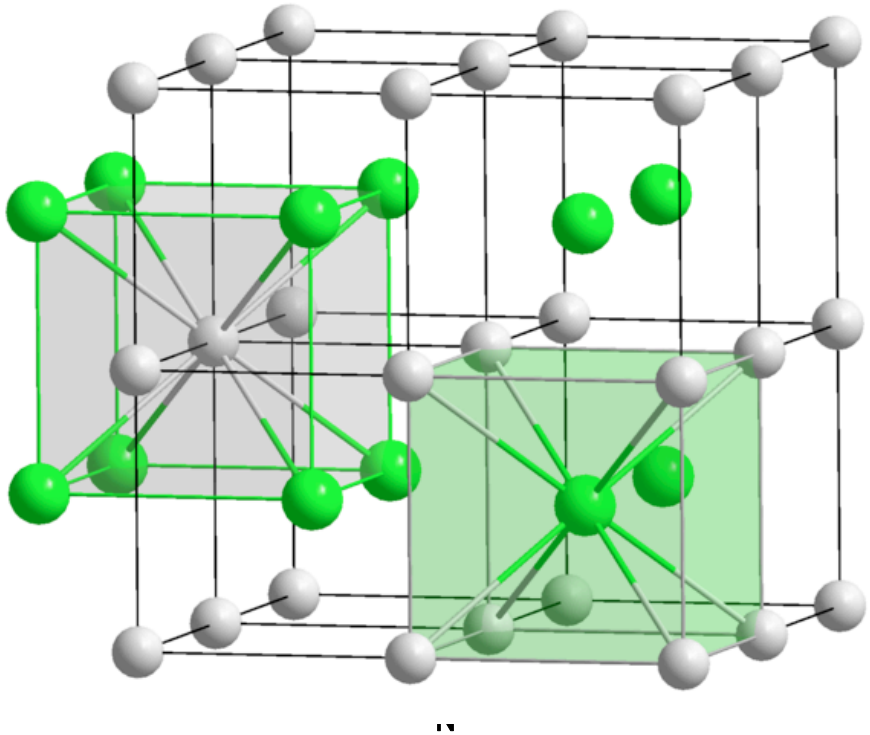

Ref: PRL **91** 165001 (2003)

Coulomb crystals of two species with the same charge-to mass ratio

Potential Exp.: 50:50 systems of $^{24}Mg^{+}$ and $^{48}Ca^{2+}$

More extreme cases, e.g.:

$^{9}Be^{+}$ - $^{27}Al^{3+}$, $^{36}Ar^{4+}$, $^{45}Sc^{5+}$, $^{54}Fe^{6+}$,..., $^{180}Hf^{20+}$, $^{189}Os^{21+}$,...

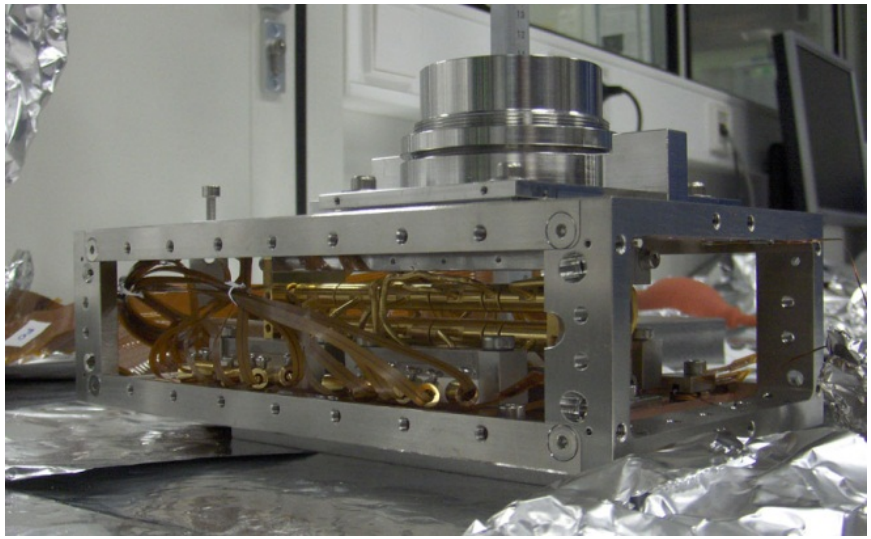

... the sensitivity of the mixing on the charge-to-mass ratio...

...one per thousand is enough to observe at least partial segregation of the two species.

Ref: PRL **91** 165001 (2003)

This can be tested experimentally!

White Dwarfs (revisited)

The "Sun" 5 Billion years from now!

$^{12}C^{6+}$ and $^{16}O^{8+}$

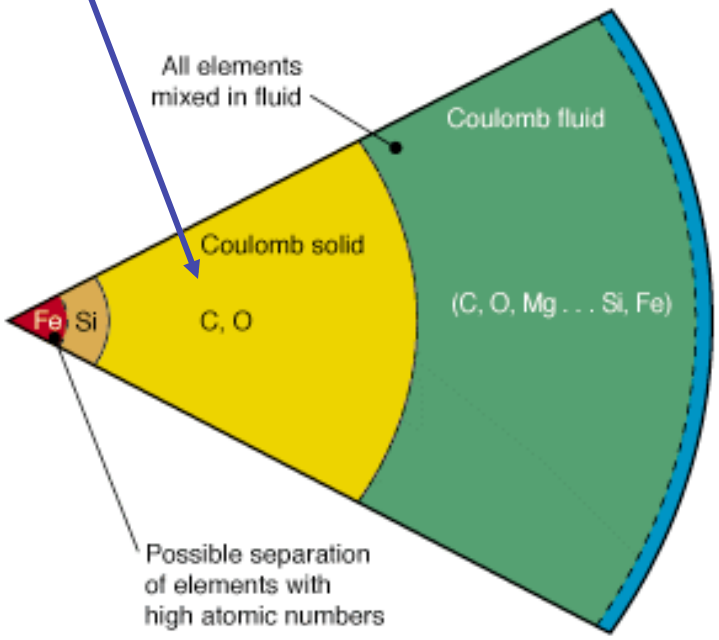

In collaboration with Piet Schmidt, PTB, and J. José R. Crespo López Urrutia, MPIK (Project leader)

$^{9}Be^{+}$ and $^{40}Ar^{13+}$

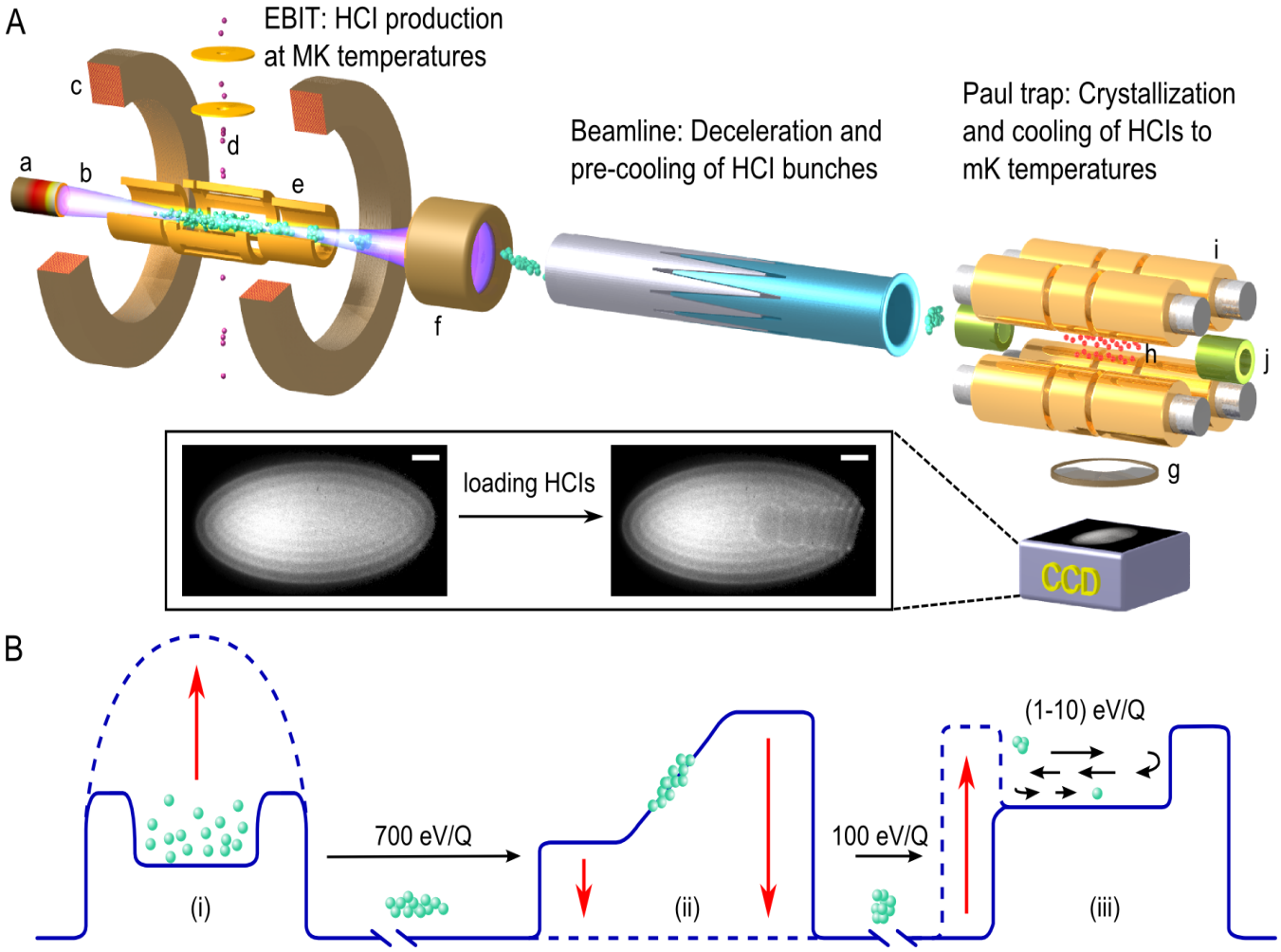

Four $^{9}Be^{+}$ and one $^{40}Ar^{13+}$ ions

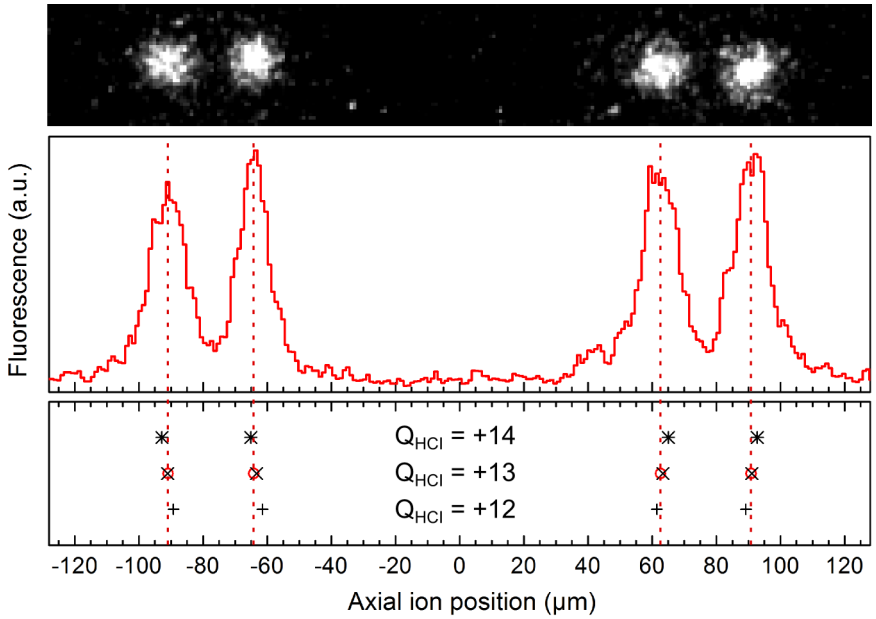

III. Metastable long-range-ordered Coulomb clusters

Observed structures in a linear Paul trap

Number of $^{40}Ca^{+}$ ions ~2700

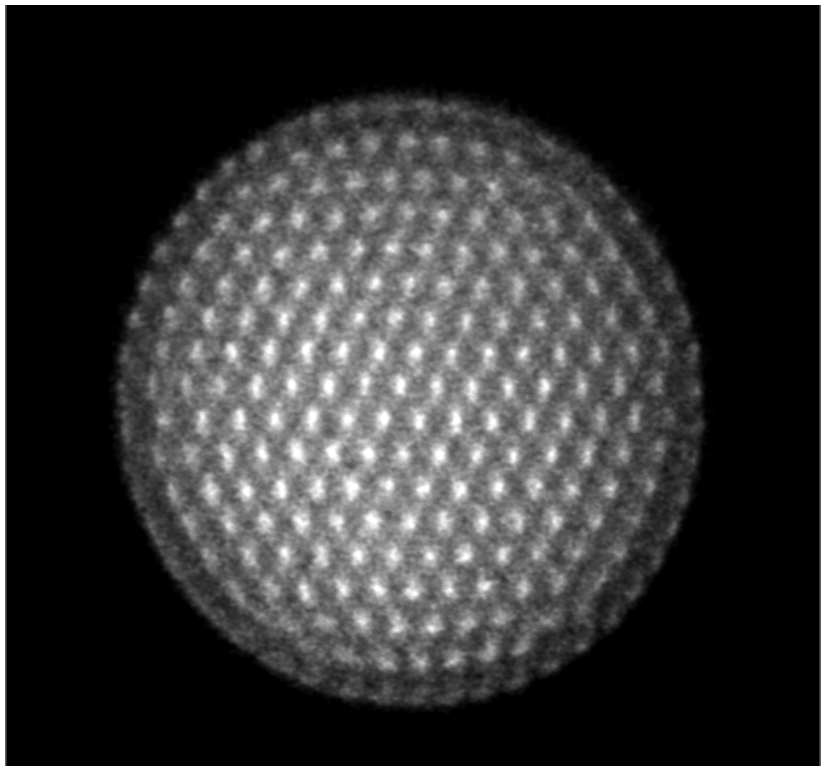

~300 μm

Cubic structures viewed along one of the <111> directions:

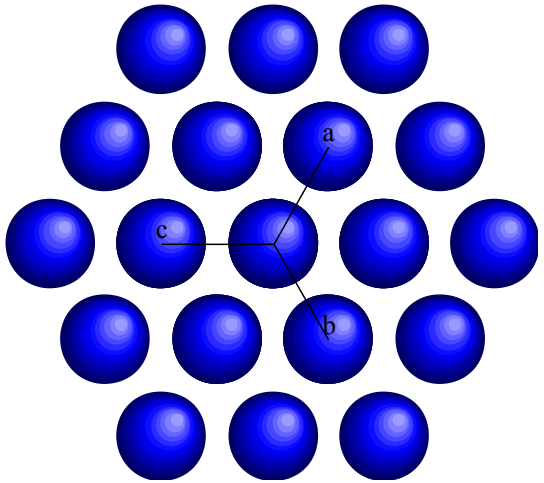

The structures are the same, BUT densities different!

($n_{bcc}=2n_{sc}=4n_{fcc}$)

Expected ion density: $n_{ions}=2.4\pm2\times10^{8}$ cm^{-3}

Ion density assuming bcc structure: $n_{bcc}=2.3\pm2\times10^{8}$ cm^{-3}

PRL **96**, 103001 (2006)

3D Long-range-order (theory)

Theory: Wigner, Hansen, Pollock, Dubin, Hasse, Totsuji, ...

Recent MD simulations:

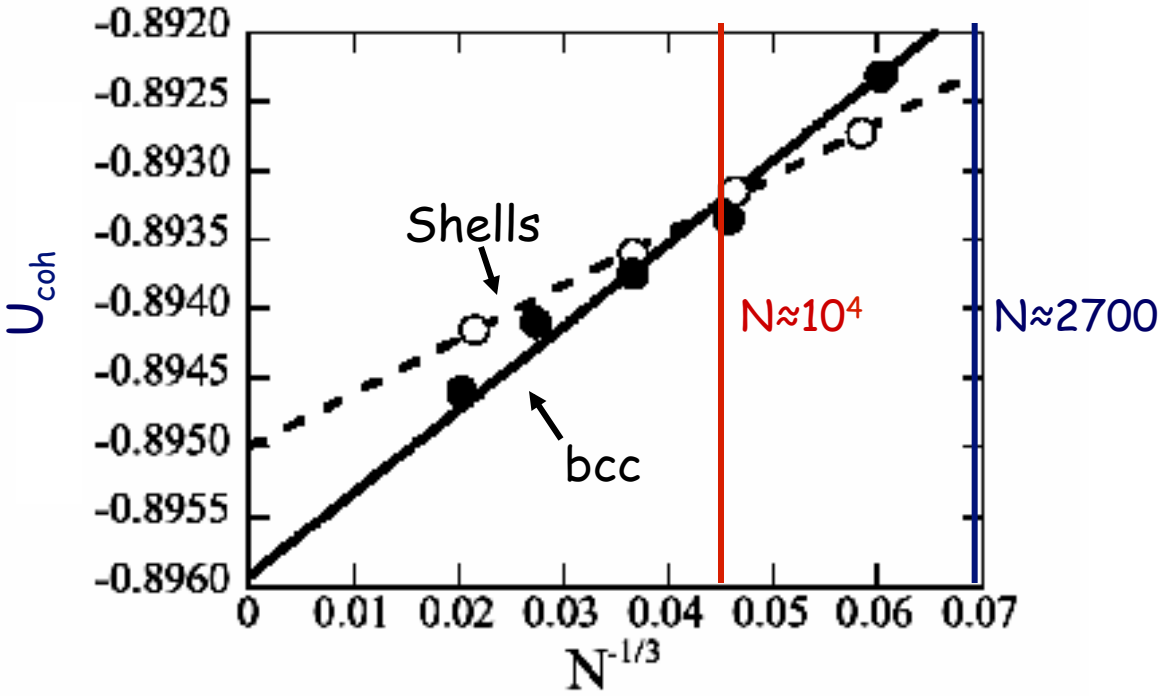

Cohesive energy: $U_{coh}=\Delta U_{sys}/(Nq^2/a)$

Ref: Totsuji *et al.*, PRL **88** 125002 (2002)

MD simulations of spherical clusters with fixed central bcc-structures

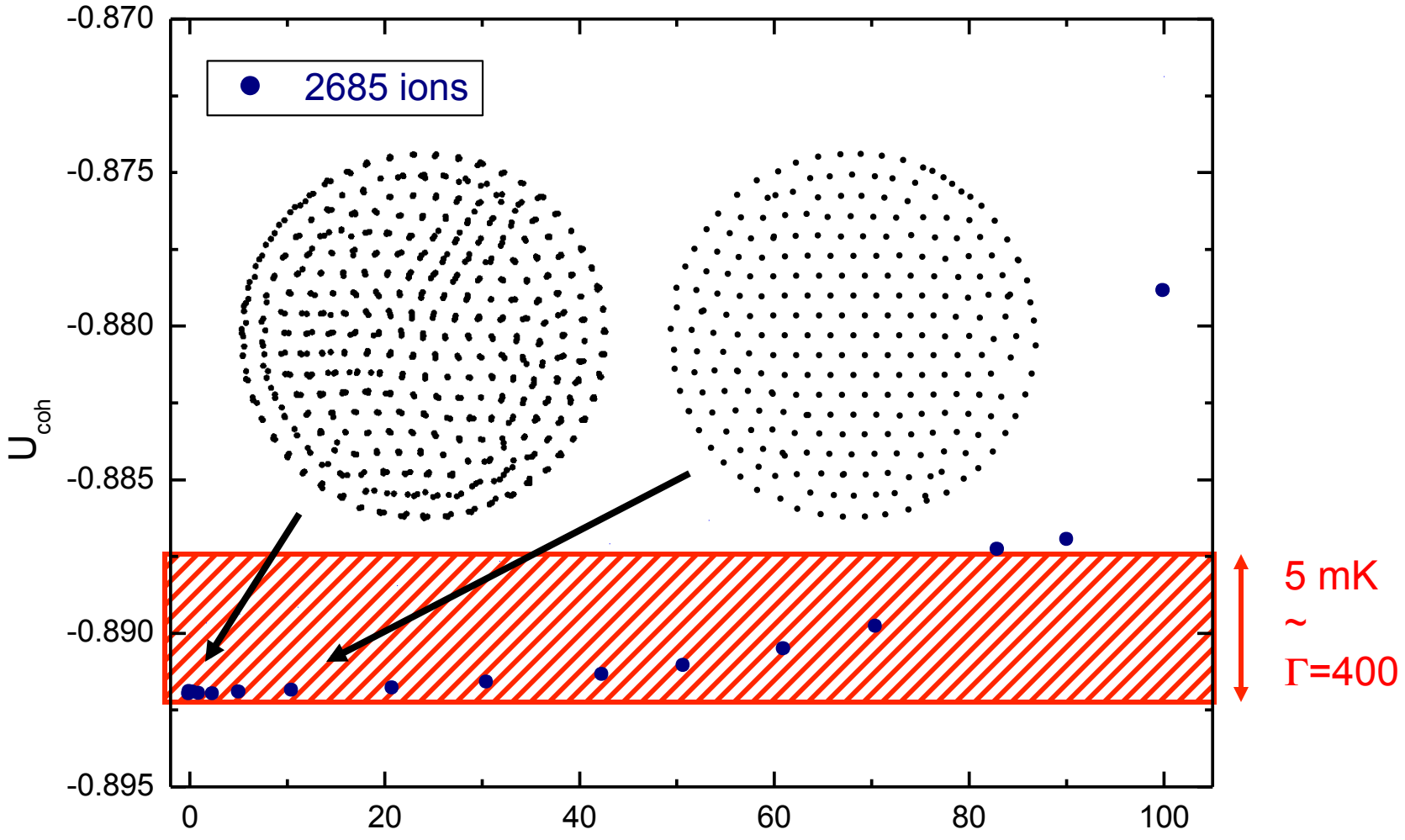

(Γ_{final} > 10.000 in all simulations)

MD simulation

2685 ions, T=1 mK (Γ~2000)

Video: 10 ms real time

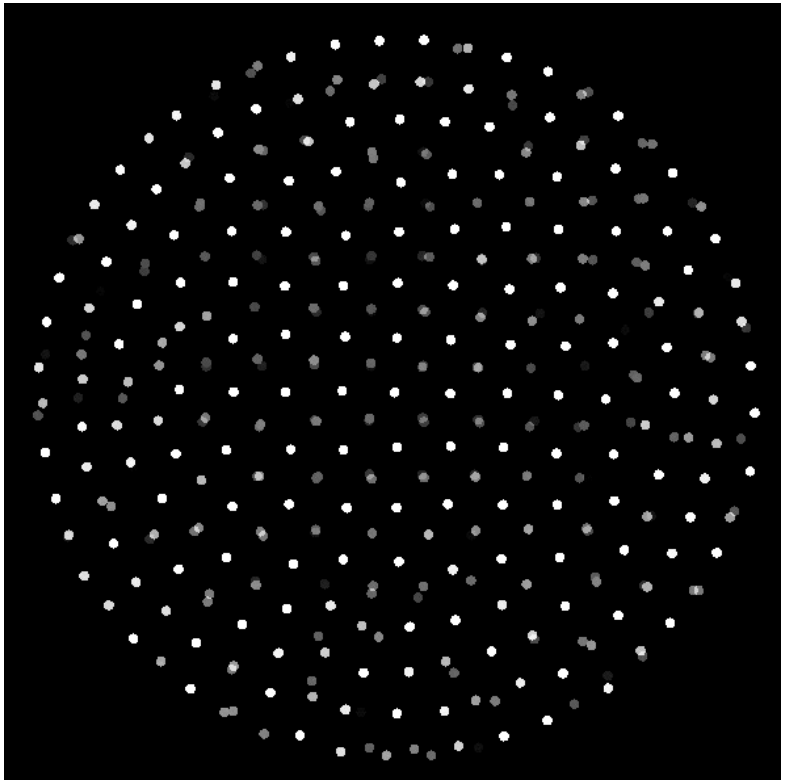

Averaged ion distribution (10 ms)

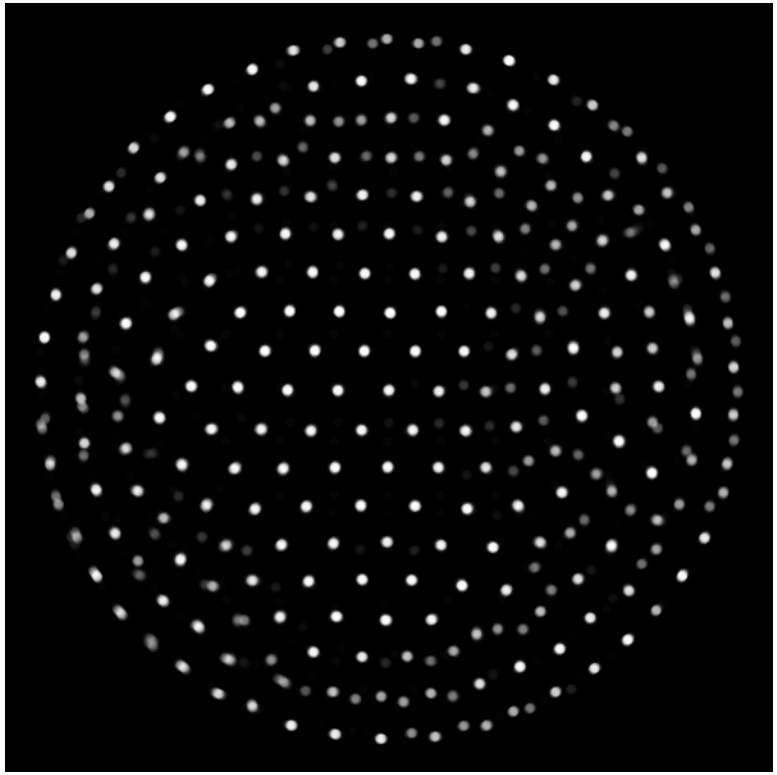

MD simulation

2685 ions, T=20 mK (Γ~100)

Video: 10 ms real time

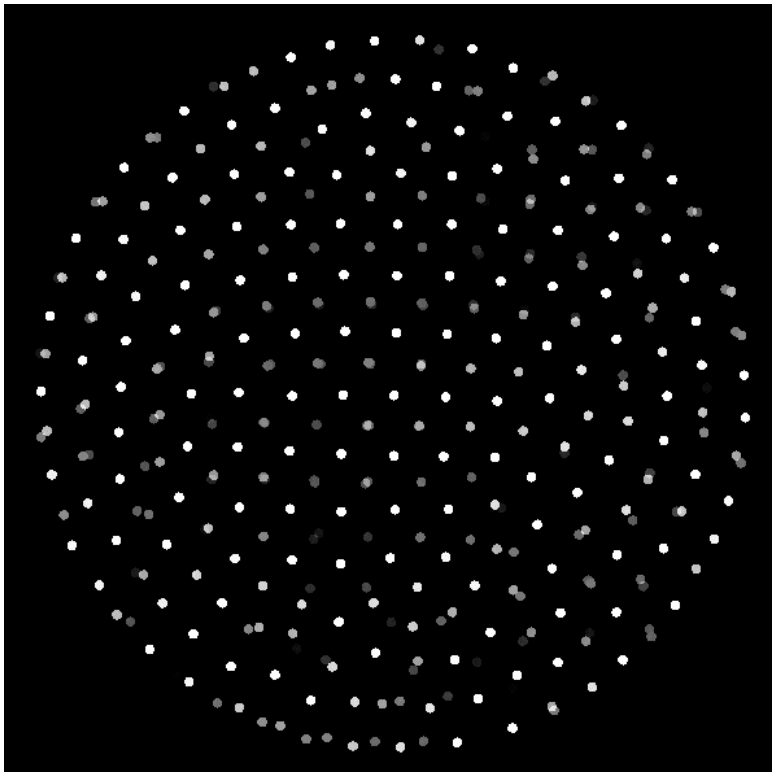

Averaged ion distribution (10 ms)

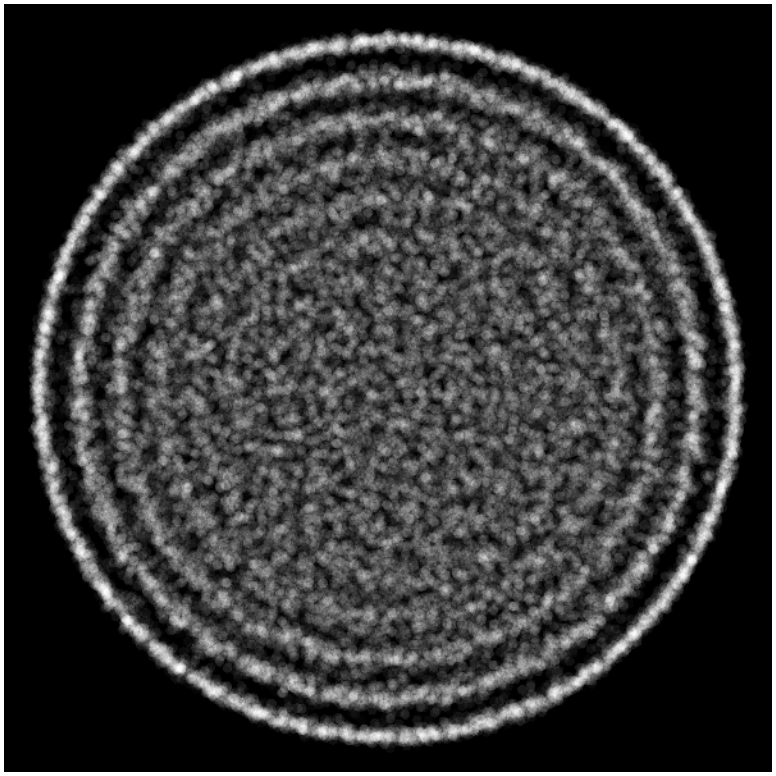

Real-time video

Number of ions: ~2500

"Snap-shots"

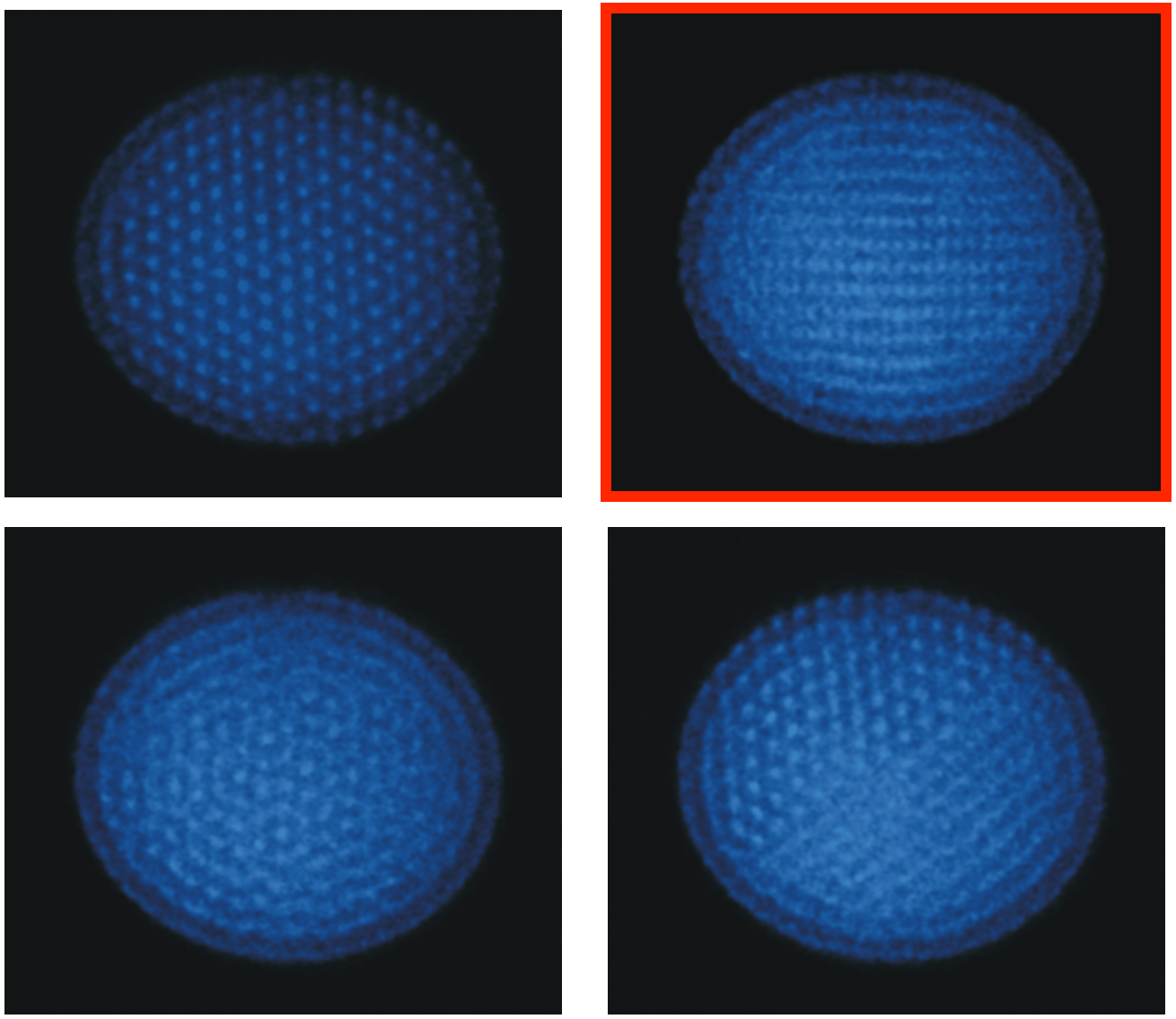

1 frame = 100 ms ≈ 10^4 τ_{osc}

arXiv:1202.2544 (2012)

FCC structure

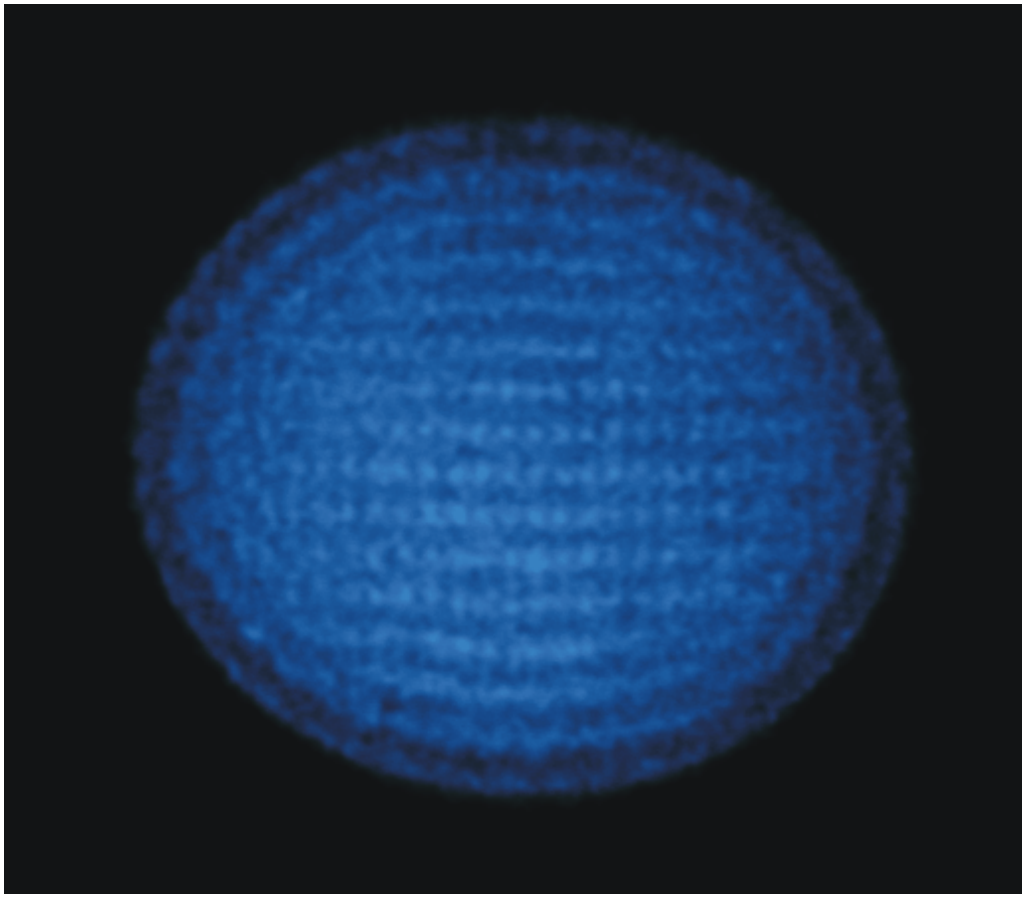

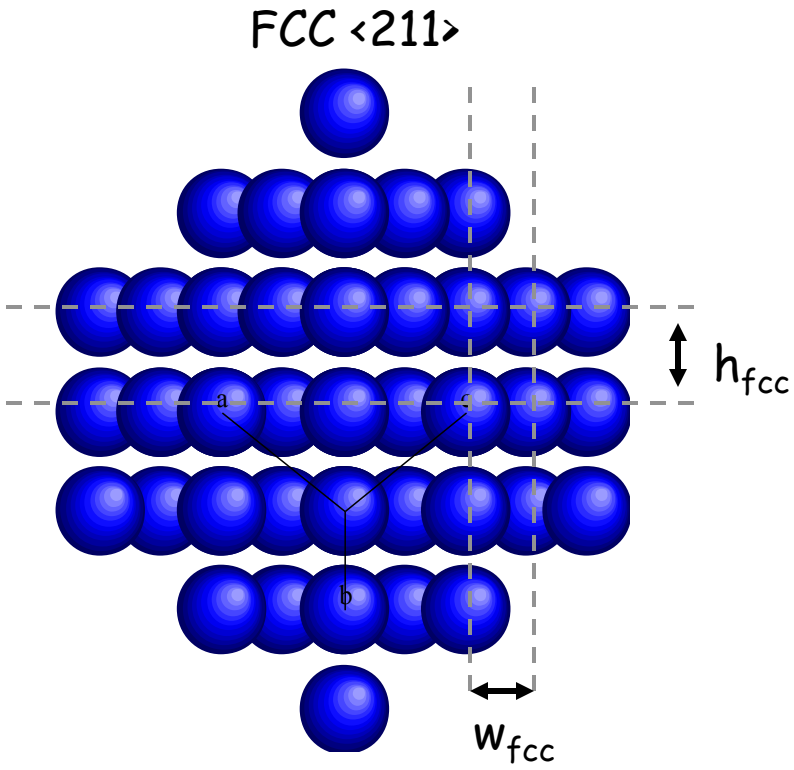

$h_{fcc}/w_{fcc} = 2^{3/2}/3^{1/2} = 1.63$

"Snap-shots"

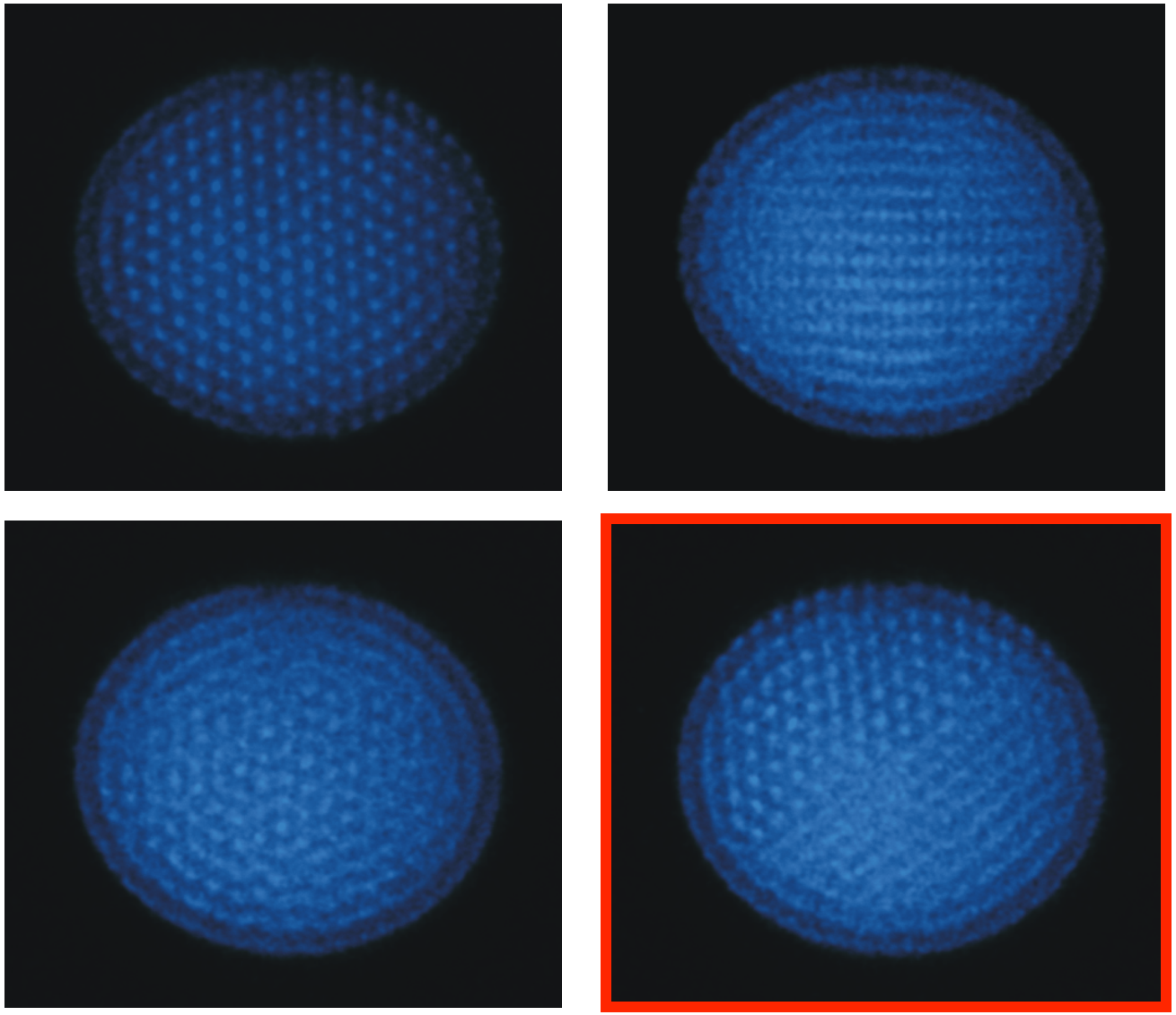

1 frame = 100 ms ≈ 10^4 τ_{osc}

arXiv:1202.2544 (2012)

BCC <110>- FCC <111> interface

Interface viewed along the <111> direction of the bcc structure

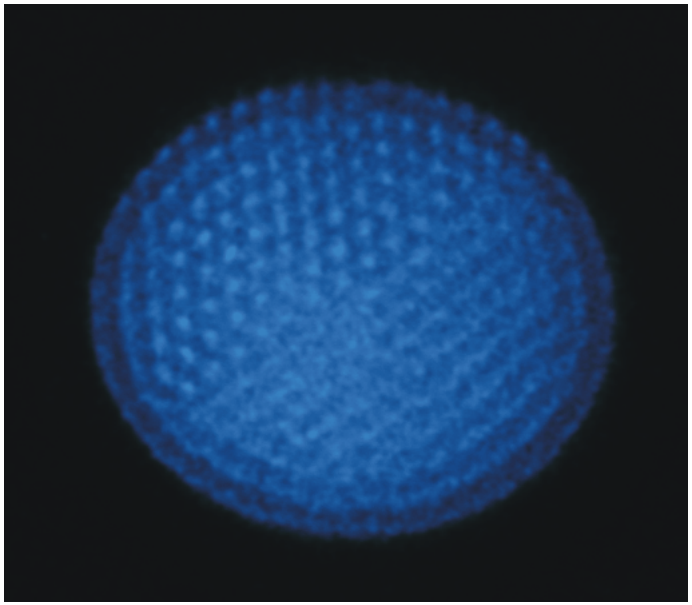

Kurdjumov-Sachs

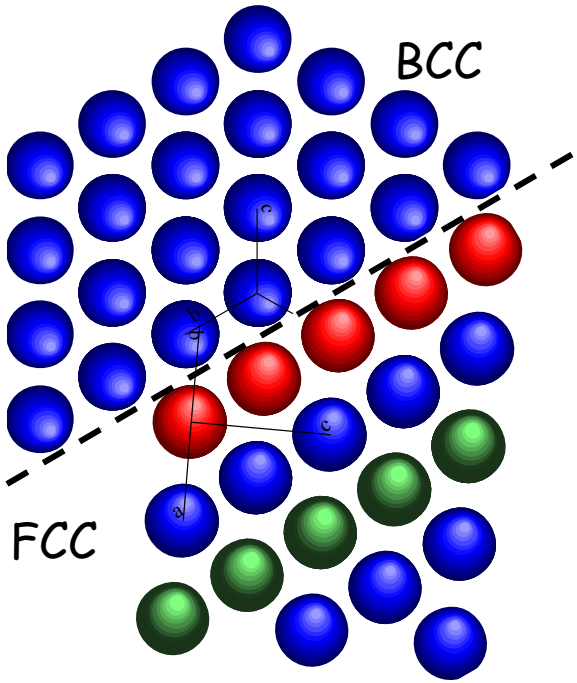

Nischiyama-Wassermann

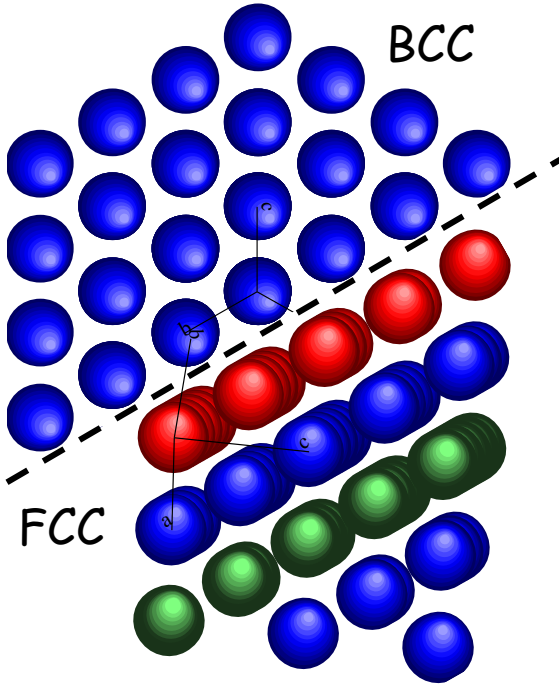

Fcc <111> - bcc <110> interface also observed in Penning traps?

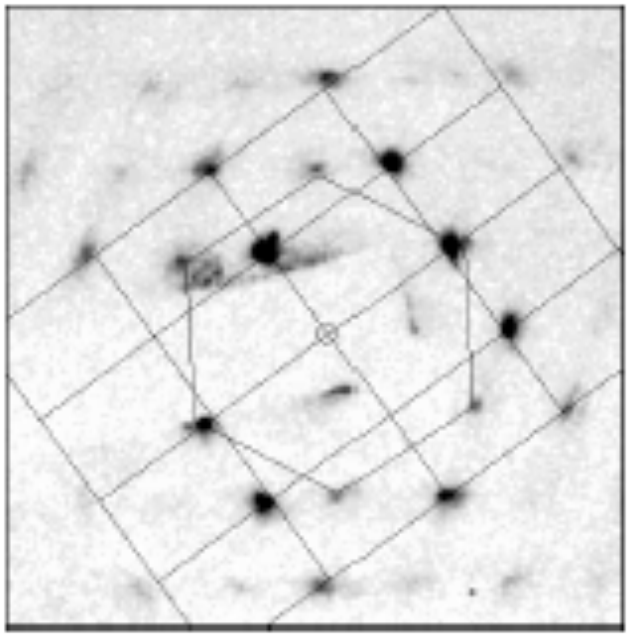

Fig. 6. Time-resolved Bragg diffraction pattern showing a superposition of twofold and sixfold symmetric patterns. The rectangular grid connects the points for which diffraction spots are predicted for a bcc lattice oriented along a ⟨110⟩ direction. An fcc lattice oriented along a ⟨111⟩ direction would generate diffraction spots at the vertices of the hexagon. The orientation of the hexagon has been adjusted to fit the data, and it differs by about 3° from that of the rectangular grid. The active timing method and the CCD camera were used. Here, $\omega_r = 2\pi \times 70$ kHz, $n_0 = 2.15 \times 10^8$ cm^{-3}, $N = 5 \times 10^5$, and $2r_0 = 2.27$ mm.

Expected orientation:

Kurdjumov-Sachs:

5.3°

Nischiyama-Wassermann

0°

Penning trap experiment

3°

W. M. Itano *et al.*, Science **279**, 686 (1998)

IV. Control of crystal structures by light induced forces

Introduction to optically induced potentials

Generally, we can polarize atoms/ions:

$$\tilde{p} = \alpha \tilde{E} \qquad \Rightarrow \qquad U_{\mathrm{dip}} = -\frac{1}{2}\langle \mathbf{pE} \rangle = -\frac{1}{2\epsilon_0 c}\mathrm{Re}(\alpha)\, I$$

Two level atom/ion:

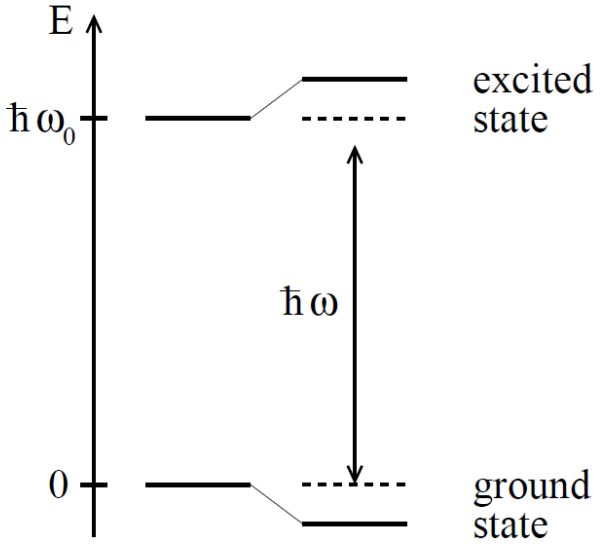

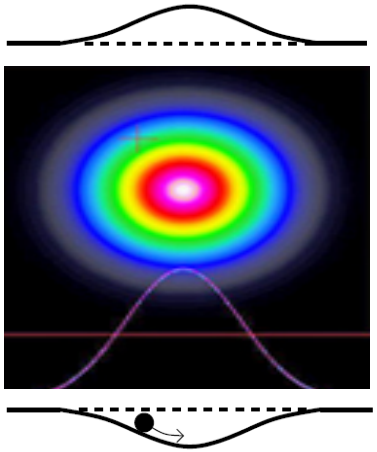

$$U_{\mathrm{dip}}(\mathbf{r}) = \frac{3\pi c^2}{2\omega_0^3}\frac{\Gamma}{\Delta} I(\mathbf{r})$$

$$\Delta \equiv \omega - \omega_0$$

Exploitation of optically induced potentials

A) Control of structural phases of Coulomb crystals

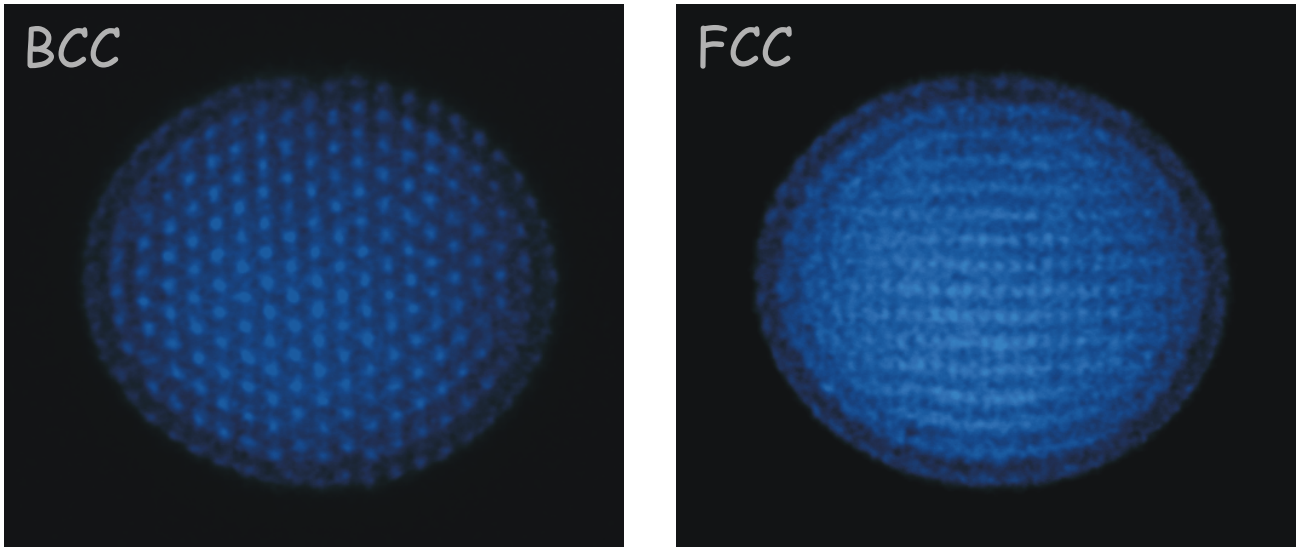

Idea:

Try to clamp specific lattice planes by standing wave optical fields.

Standing wave field induced potential

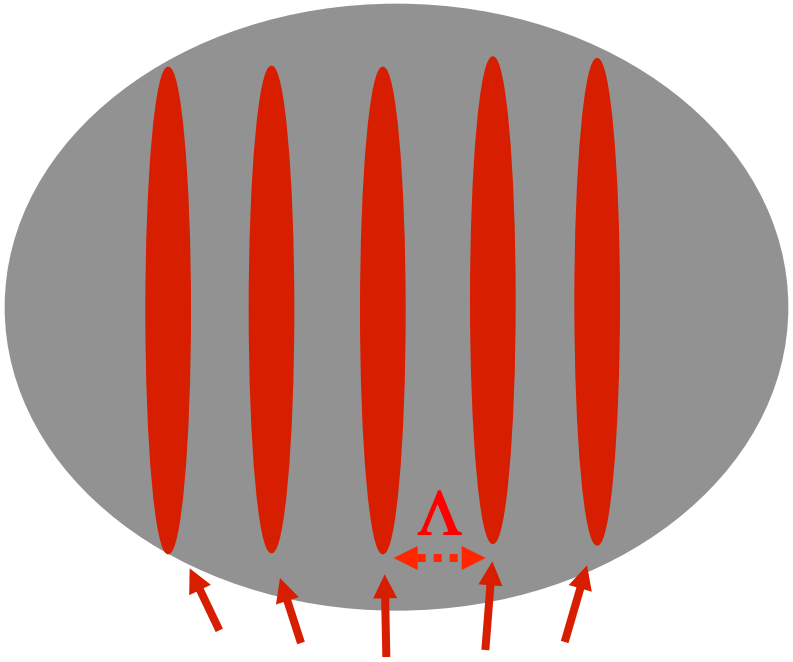

Interference pattern from two crossing light beams

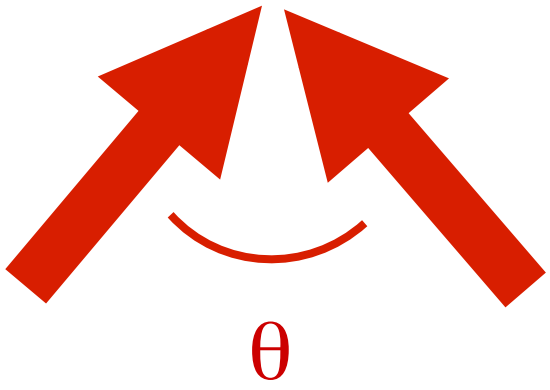

Standing wave period Λ can be controlled by the angle θ

MD simulation results with 1000 ions

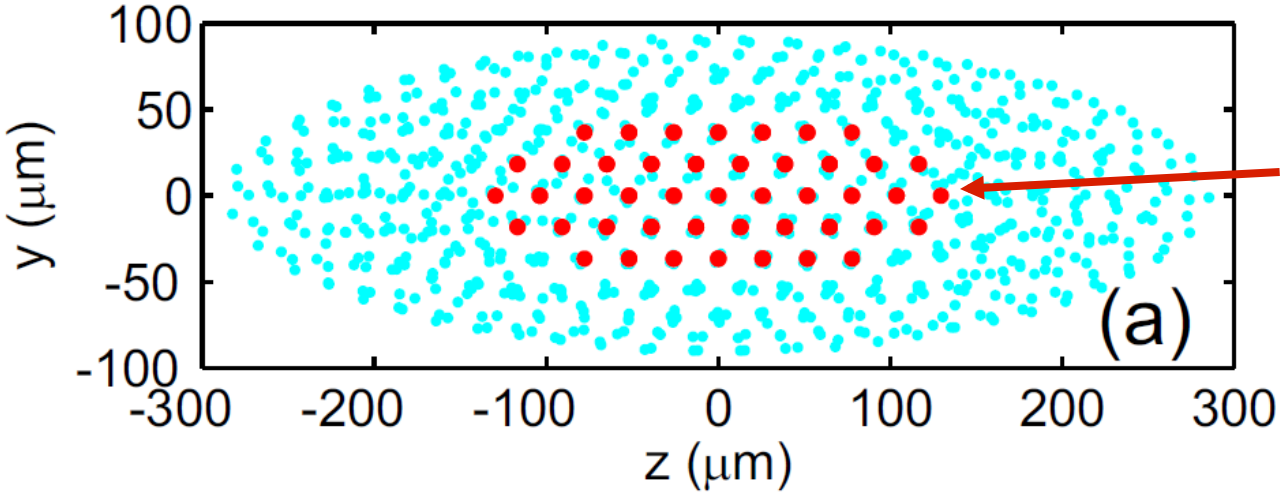

64 ions initially fixed in a fcc structure

Next, release the initially fixed ions, and see if they stay:

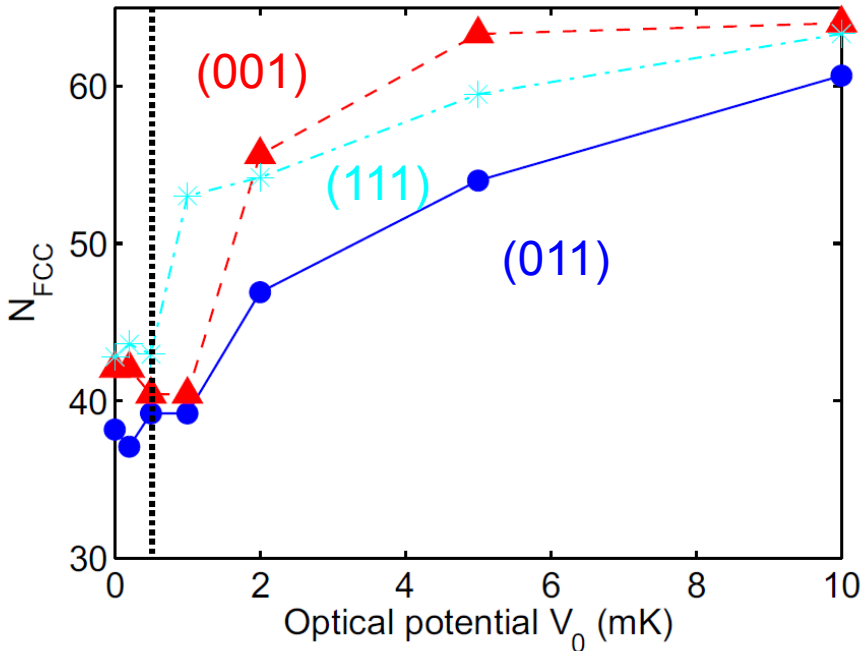

P. Horak, A. Dantan, and M. Drewsen, Phys. Rev. A **86**, 043435 (2012)

Can we induce a structural phase transition?

BCC <110>- FCC <111> interface

Interface viewed along the <111> direction of the bcc structure

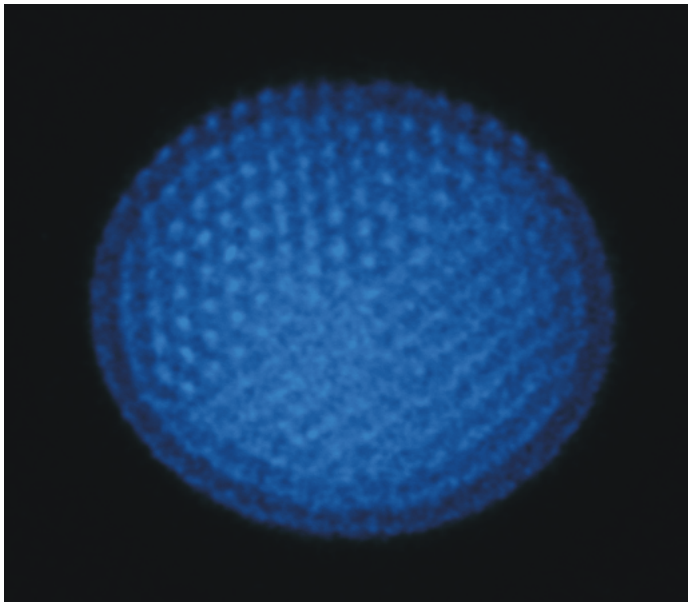

Kurdjumov-Sachs

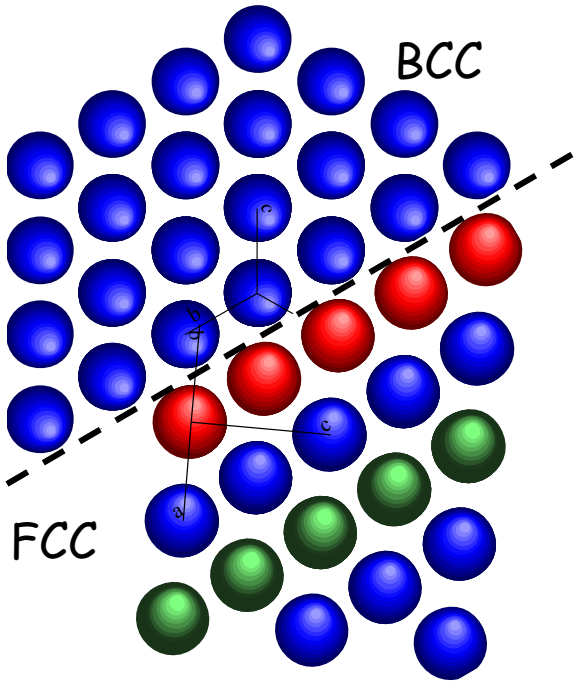

Nischiyama-Wassermann

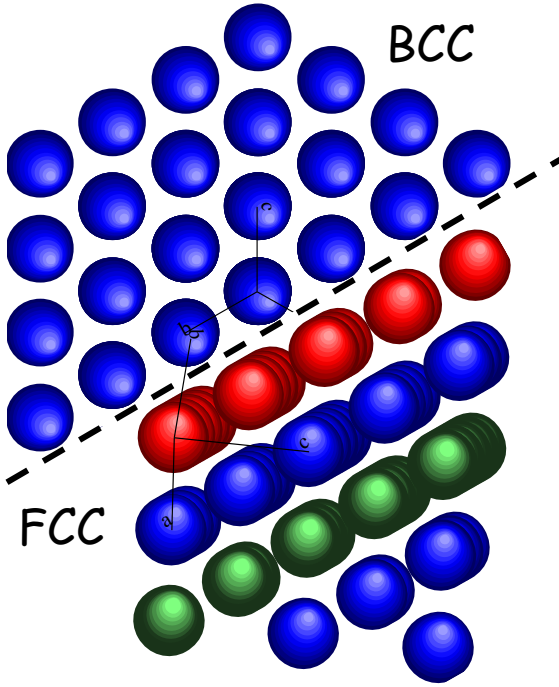

Can we induce a structural phase transition?

The Bain path:

fcc ⟷ bcc

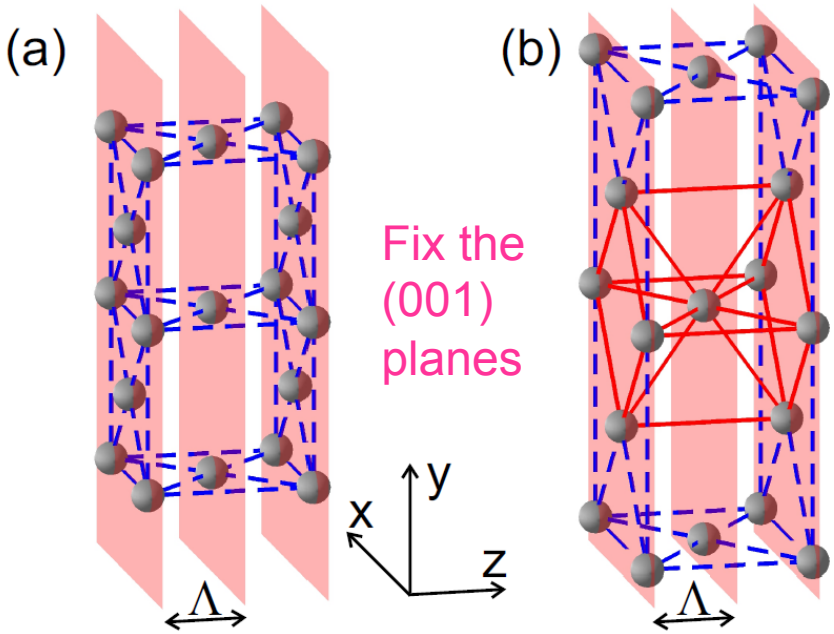

Keeps the number of particles in planes constant, but changes the density by a factor of 2 !

Can this be achieved experimentally?

Seems so:

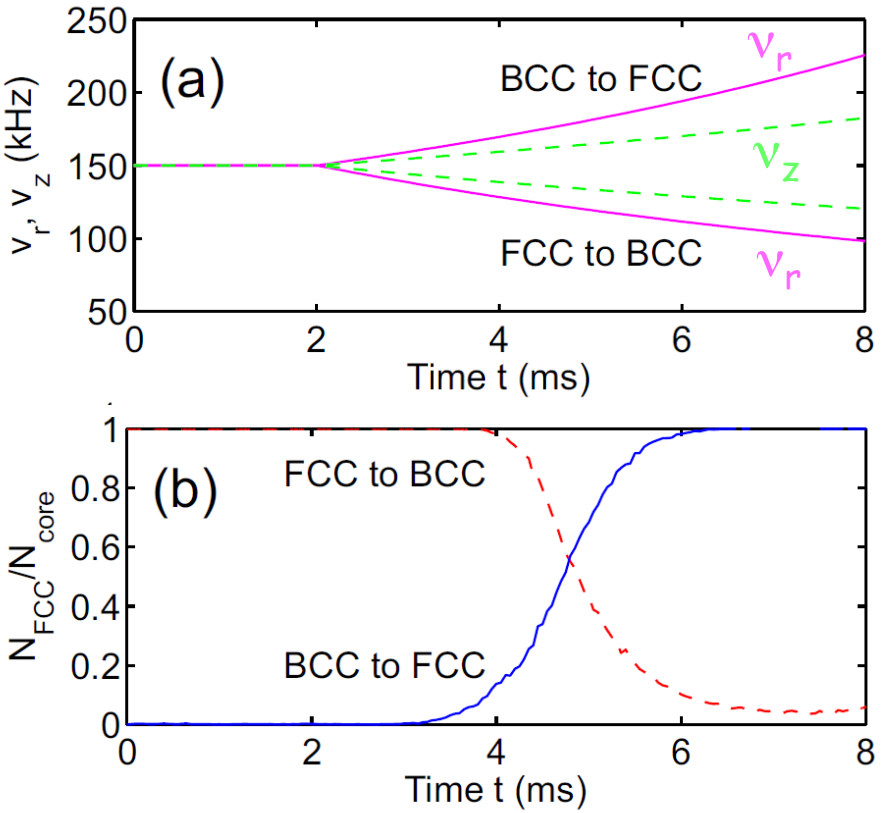

P. Horak, A. Dantan, and M. Drewsen, Phys. Rev. A **86**, 043435 (2012)